FLUCTUATIONS IN SOIL MICROBIAL COMMUNITIES AND CO-OCCURRENCE NETWORKS AT VARIOUS GROWTH STAGES OF *ARTEMISIA ANNUAL* L.

CHU YANG[1†], HONG-HAO HUO[2†], SHI-QIONG LUO[1*] AND ZHAN-NAN YANG[2*]

[1] School of Life Sciences, Guizhou Normal University, Guizhou Guiyang, China
[2] Key Laboratory for Mountainous Environment Information and Ecological Protection of Guizhou Province, Guizhou Normal University, Guizhou Guiyang, China

*Corresponding author's email: shiqiongluo@163.com, yangzhannan@163.com
[†]Chu Yang and Hong-hao Huo are co-first-author and contributed equally to this work

Abstract

Artemisia annua L. has received substantial attention as a source of the antimalarial compound, artemisinin, with the maximum content being observed during the squaring (bud emergence) period. However, dynamic fluctuations in microbial communities and co-occurrence networks in the soil of *A. annua* during plant growth remain unclear. In this study, pot experiments were performed using *A. annua* from two provenances to analyze its growth and major bioactive components to elucidate the responses of plant-associated indices and soil microbial communities (SMCs) at different growth stages of the plant. Furthermore, correlations between SMCs and *A. annua* growth parameters were explored. The results revealed that the activities of three soil enzymes (phosphatase, sucrase, and urease), plant height, branch numbers, as well as artemisinin and total polyphenol contents were increased with the progression of *A. annua* growth. However, soil physicochemical properties exhibited a contrasting trend. As *A. annua* growth progressed, the richness and diversity of soil bacteria generally decreased, whereas those of soil fungi increased, and microbial co-occurrence networks became less complex. Microbial communities fluctuated to varying degrees during the pot-culture process. Proteobacteria (31.5–48.4%) and Ascomycota (21.9–84.1%) accounted for the highest ratio of bacteria and fungi phyla, respectively, and had the maximum bacterial and fungal abundances during the nutritional flourish and flower bud differentiation stages of *A. annua*, respectively. Some SMCs were significantly positively or negatively ($p \leq 0.5$) correlated with plant growth parameters and major bioactive components of *A. annua*. Some microbial communities closely interplayed with soil physicochemical traits and enzyme activities. Our results provide evidence that SMCs in the soil of *A. annua* vary at different growth stages, and are closely correlated with plant fitness and artemisinin content.

Key words: *Artemisia annua* L.; Provenance; Microbial community; Co-occurrence network; Active component; Plant growth

Introduction

Plant growth is closely associated with abiotic and biotic factors, including soil microbes and environmentally physicochemical property. Plant growth characteristics are largely determined by the phylogenetic species identity (Roscher *et al*., 2013), as well as biotic and abiotic soil components, including soil microorganisms, types and activities of various enzymes, soil pH, organic matter, nutrient availability, among others (Bergmann *et al*., 2016; Bjørnlund *et al*., 2012; Xie *et al*., 2022; Ordoñez *et al*., 2010). The enhancement in root exudates during plant growth, and decomposition of dead twigs and withered leaves alter biotic and abiotic soil properties (Yuan *et al*., 2017; Coskun *et al*., 2017; Clarholm *et al*., 2015; Nguyen, 2003). As a key constituent of the soil ecosystem, microbes facilitate the degradation of organic matter and conversion and utilization of nitrogen (N), phosphorus (P), sulfur (S), and other nutrients (Philippot *et al*., 2023). Thus, soil microbes form intimate relationships with plants, and the other way round, which affect the plant ability to absorb nutrients, water, and overcome environmental challenging (Bardgett & Van der Putten, 2014; Van der Heijden *et al*., 2008). In addition, the interplays between SMCs and plants affect plant growth or the synthesis of some bioactive components, which enhance plant tolerance to stresses and plant fitness (Petipas *et al*., 2021; Lau & Lennon, 2012; Luo *et al*., 2014). Soil microbes and plants can partially absorb nutrient elements (e.g. carbon [C], N, and P) and secrete extracellular enzymes catalyzing organic matter degradation in the plant soil. Extracellular enzymes, which are excreted by plant roots and soil microbes into soil, are referred to as soil enzymes and are indicators of soil fertility and ecological functions (Guan, 1986).

Artemisia annua L., one of the commonly used traditional Chinese herbal medicines is an annual herb belonging to the Asteraceae family. The plant has been applied as herbal medicine for more than 2000 years, with the major bioactive compound (artemisinin) being used for detoxification and heat clearing (Anon., 2020). Artemisinin has been extracted as a raw medicinal material since its isolation from *A. annua* in the 1970s by a Chinese scientist, Youyou Tu (Liao, 2009). Presently, approximately 40% of the global population is threatened by malaria; therefore, artemisinin combined therapy is still proposed by the World Health Organization (Anon., 2018) as a first-line antimalarial drug. Several wild populations of *A. annua* are distributed in Southwest China, which is the main production area of the medicinal herb (Shi *et al*., 2021; Luo *et al*., 2019a). Similar to a variety of plant species, such as

Avena barata L., *Microstegium vimineum* (Trin.) A. Camus (Goldsmith *et al*., 2023), *Ageratina adenophora* (Sprengel) King and Robinson (Poudel *et al*., 2019), *Berberis thunbergii* DC (Kourtev *et al*., 2003), *Solidago canadensis* L. (Likhanov *et al*., 2021), *Bromus secalinus* L. (Pytlarz & Gala-Czekaj, 2022) that invade wilderness areas, *A. annua* can form a dominant community in rocky desertification areas with poor soils and it contributes to the prevention of soil erosion, and mitigation of environmental degradation (Luo *et al*., 2019b; Luo *et al*., 2014). The biomass of microbes in the rhizosphere soil (RS) of wild *A. annua* has been shown to be significantly correlated with artemisinin and artemisinic acid contents (Luo *et al*., 2014). A previous study on a seven-year plantation history of *A. annua* revealed that microbial networks in RS were less complex than those in bulk and unplanted soils. The abundances of bacterial genera *Sphingobium* and *Sphingomonas*, and saprotrophic fungi in the RS are enriched (Shi *et al*., 2021). However, a few studies have investigated variations in SMCs and their networks in the RS of *A. annua* during its growth.

Our work was designed to investigate fluctuation in SMC structure and composition, soil properties and enzyme activities, plant growth and major bioactive components in leaves, as well as correlations between SMCs and plant traits at different growth stages of *A. annua*. Specifically, this work aimed to determine the following: (1) variations in the SMC diversity, structure, and composition with the progression in *A. annua* growth; (2) whether the interactional networks of SMCs become more complex with the progression of *A. annua* growth; (3) whether soil microbes are associated with *A. annua* growth and its major bioactive components. The findings of this work will promote our understanding of fluctuations and co-occurrence networks in SMCs at different growth stages of *A. annua*, and the correlations between SMCs and plant agronomic traits. It is helpful to understand the close relationship between soil microbes and artemisinin, the unique active ingredient of this plant species.

Materials and Methods

Collection of *A. annua* seeds: Wild *A. annua* seeds were collected from mature plants in two provenances in Guizhou Province of China, between November and December. Provenance I was Gaotun (GT) in Liping County, which is located in the southeast region of Guizhou Province, China (26°68′75″ N, 109°18′81″ E; altitude of 440 m above sea level [a.s.l.]) and provenance II was Jiuchang (JC) in Guiyang City, which is the provincial capital of Guizhou Province, China (26°91′09″ N, 106°68′75″ E; altitude of 1329 m a.s.l.). Healthy wild seeds of *A. annua*, from a strong plant with many branches, were collected from each location, dried under a shade, and stored for subsequent pot cultivation experiments. These seeds were subjected to purification and warm-water soaking before sowing. Specifically, purification was performed to remove the impurities and inferior seeds to ensure the seed purity, then the purified seeds were put into a white cloth-bag and soaked in warm-water at 50ºC for half an hour in order to disinfection, during which the seeds were continuously stirred, the bag with seeds was taken out and soaked in clean-water for 24 h, which ensured the seeds could break the hard shell and promoted water absorption and germination.

Pot experiments: Pot cultivation experiments were conducted in a greenhouse at the Guizhou Key Laboratory, Guizhou Normal University, Guiyang city, China. To meet the nutritional requirements of plant growth and explore the variation of soil nutrient in the plant rhizosphere, the soil used for the pot experiments was natural organic soil purchased from a local flower market, Ali Hill in Guiyang City of Guizhou Province, China. Soil pH was 7.4, available phosphorus (AP) was 128.9 mg kg^{-1}, organic matter (OM) was 99.0 g kg^{-1}, available potassium (AK) was 117.4 mg kg^{-1}, and available nitrogen (AN) was 223.4 mg kg^{-1}. Approximately 100 treated seeds mixed with fine sand were sowed in polyethylene pots (30 cm in diameter and 40 cm in height) containing 15 kg of dry natural organic soil on April 10, with each provenance having three pots (a total of six pots), which were watered regularly. After the seedlings grew to a height of 20 cm, they were transplanted into pots (diameter 30 cm, height 40 cm) containing 15 kg of dry natural organic soil (15 replicate pots for each provenance, totaling 30 pots). A plant seedling per pot, the seedlings were watered and weeded regularly, but no any fertilizers were added, exposed to natural light, temperature, and humidity. it is subtropical humid monsoon climate. The mean annual temperature is approximately 15.3°C, mean annual relative humidity is 77%, the mean annual sunshine duration was 1160 h.

Sample collection and treatments: The growth stages of *A. annua* were as follows: seed treatment (ST, sowing, control soil in this experiment), seedling stage (SS, 15 d after the *A. annua* seedlings were planted into pots), nutritional flourish (NF), flower bud differentiation (FBD), and squaring period (SP). To avoid damaging plant roots, soil was collected at 5 cm away from the base of plant stem using an auger (Xie *et al*., 2022). Because the roots of *A. annua* are well developed, and the fibrous roots are abundant and distributed throughout the pot. In the nature state, the lateral root can reach 30 cm from *A. annua* stem base. The samplings were collected non-destructively, so the sampling soils were considered as the rhizosphere soils (RS) from *A. annua* seedling (Luo *et al*., 2014). Soil samples in three pots with plants were considered a replicate at the time of sampling. The RS samples were mixed and transferred into sterile plastic bags, three replicates for each provenance. After transporting the soil samples to the laboratory, stones, plant residues, and other debris were removed on an ultra-clean table. We divided each soil sample into two-portion half: a portion (5 g) was put into a plastic sterile bag and kept at -80°C for high-throughput sequencing of SMCs, while another portion was naturally air-dried on kraft papers for chemical analysis of soil physicochemical traits and enzymatic activity. The mature leaves from the middle and lower parts of *A. annua* plants were sampled during each growth stage and placed at 4°C for the assay of artemisinin and total polyphenol contents. Three pots with plants were considered a replicate, three repetitions for plant samples from each provenance.

Determination of soil physicochemical traits and enzyme activities: Soil physicochemical traits were tested according to the Bao's methods (2000). Soil pH was tested in a suspension of water and soil (2.5:1, v/w) using a glass electrode (PHS-3E; Lei-Ci Scientific Instruments Co., Ltd., Shanghai, China). Soil OM concentration was analyzed by

titration after oxidation of RS samples with a mixed liquid of concentrated sulfuric acid and potassium dichromate; AN was determined using the boric acid titration method; AP was determined by molybdenum blue spectrophotometry (759S ultraviolet-visible spectrophotometer; Lengguang Technology Co., Ltd., Shanghai, China); AK was determined by flame photometry (BDN900 flame photometer; Bell Analytical Instruments Co., Ltd., Dalian, China).

Soil enzymatic activities were analyzed in accordance with Guan's methods (1986). Urease activity (URA) was measured by phenol-sodium hypochlorite colorimetry. Air-dried soil (5 g) was mixed with a buffer solution (pH 6.7) containing citric acid and potassium hydroxide. Afterward, urea was added as a reaction substrate and the solution was incubated at 37°C for 24 h. The quantity of ammonium N (NH_4^+-N) formed was determined by spectrophotometry at a 578 nm wavelength to analyze URA (mg NH_4^+-N g^{-1} 24 h^{-1}). Phosphatase activity (PHA) was tested by disodium phenyl phosphate (DPP) colorimetry. Soil samples were mixed with a buffer solution (pH 5.0, when the soil pH was less than 7.0) containing acetate or borate (pH 9.4, when the soil pH was greater than 7.0). Disodium phenyl phosphate was added as a reaction substrate, leading to the formation of a phenol whose absorbance value was measured at a 660 nm wavelength to determine PHA (mg phenol g^{-1} 24 h^{-1}). 3,5-dinitrosalicylic acid colorimetry was applied to analyze sucrase activity (SUA). Soil samples were mixed with a buffer solution containing $Na_2HPO_4 \cdot H_2O$ and KH_2PO_4, followed by the addition of saccharose as a reaction substrate. The absorbance value of the glucose produced was tested by spectrophotometry at 508 nm to analyze SUA (mg glucose g^{-1} 24 h^{-1}). Soil used for the quantitative analysis of the three soil enzymatic activities weighed approximately 5 g. The soil samples were mixed with specific buffer solutions and then incubated for 24 h at 37°C.

Measurement of plant growth parameters and contents of major bioactive components: Plant growth parameters, including plant height and branch numbers were measured at each growth stage of *A. annua*. The major bioactive components (artemisinin and total polyphenol) of *A. annua* leaves were analyzed (Luo et al., 2019b). Fresh leaves (about 0.125 g) were cut into pieces, placed in a 5-mL bottle, and 4 mL 95% ethanol was added to the leaves. After exposure to sonic oscillation for 30 min, then the extract solution was filtered into another 5-mL bottle and put at 4°C for the quantitative analysis of artemisinin and total polyphenol contents. Total polyphenol content was determined using the Folin–Ciocalteu colorimetric method. Briefly, 1 mL ethanol extract solution was transferred into a 25-mL volumetric flask and 1 mL of Folin–Ciocalteu reagent and 2 mL Na_2CO_3 (12%) were added. The solution was then made up to 25 mL volume and left to react in darkness for 2 hours. A spectrophotometer (759S ultraviolet-visible spectrophotometer; Lengguang Technology Co., Ltd., Shanghai, China) was used to measure absorbance value of the sample solution tested at 765 nm. Artemisinin content was determined applying a gas chromatography mass spectrometer (GC–MS; GCMS-QP2010, Shimadzu) and 0.1 mg mL^{-1} artemisinin and naphthalene were used as external and interior standards, respectively. The instrument was equipped with a GC–MS solution 2.10 and chromatographic column (Zebron, ZB-1701; 30 m × 0.25 mm × 0.25 μm). The initial temperature was set to 50°C, the temperature was raised to 220°C at a rate of 15°C per minute, maintained for 5 min, then raised to 230°C at the

previously mentioned rate, and maintained for 10 min. The ion source temperature was set to 250°C, carrier gas was helium, and shunt ratio was 10:1. The m/z for artemisinin quantitative ions was 166, whereas those of qualitative ions were 137, 165, and 151. The m/z for naphthalene quantitative ions was 128, whereas those of qualitative ions were 102 and 128.

DNA extraction, amplification, and sequencing: The microbial DNA in RS samples was extracted applying E.Z.N.A Omega Mag-Bind Soil DNA Kit (Omega Bio-Tek, Norcross, GA, USA), according to the manufacturer's protocols. DNA integrity was evaluated using 1% agarose gel electrophoresis (AGE). The DNA concentrations of soil samples were measured applying a Qubit 3.0 fluorometer (Nanjing Geng Chen Scientific Instrument Co., Ltd., Nanjing, China). During the first amplification, the barcoded primers 341F (CCTACGGGNGGCWGCAG) and 806R (GGACTA CHVGGGTATCTAAT) were applied to amplify the V3–V4 region of the 16S rRNA gene of RS bacteria (Xu et al., 2017). The barcoded primers KYO2F (GATGAACGYAGYRAA) and ITS4R (TCCTCCGCTTATTGATATGC) were used to amplify the internal transcribed spacer 2 (ITS2) region of RS fungal genes (Guo et al., 2019). Illumina bridge PCR compatible primers were used to amplify DNA sequences during the second amplification. Gene library size was determined using 2% AGE and gene library concentrations were determined using Qubit 3.0 fluorometer. The purified PCR products were sequenced on an Illumina HiSeq platform (Illumina Inc. San Diego, CA, USA). Extraction, amplification, and sequencing of soil bacterial and fungal DNA were performed by Sangon Biotechnology Co., Ltd. (Shanghai, China).

The datasets of fungal and bacterial reads generated during the current work are available in the NCBI repository with the accession numbers of PRJNA1195656 for bacteria and PRJNA1195669 for fungi.

Bioinformatics and statistical analyses: Raw fungal and bacterial reads obtained from the soil of *A. annua* were processed using relevant software. Cutadapt v1.18 was used to remove primers and linkers from the paired-end sequences (Martin, 2011). It was followed by workflow including filtering, dereplication, removing of chimeric sequences, and merging of the paired end sequences through software PEAR v0.9.8 (Zhang et al., 2013; Schmieder & Edwards, 2011). Non-repetitive sequence reads were clustered using Uparse v7.1 into operational taxonomic units (OTUs) on account of the criterion of > 97% similarity (Edgar, 2013; 2016). Taxonomic assignment of microbial OTUs was performed applying RDP Classifier v2.12 against the SILVA library (http://www.arb-silva.de/) for 16S bacteria, and using Blast v2.10.0 against the UNITE library (http://unite.ut.ee/index.php) for ITS fungi (Abarenkov et al., 2010). On the end, the microbial community composition of every soil sample was calculated at each classification level (including domain, phylum, class, order, family, and genus). Mothur v1.43.0 was used to evaluate α-diversity parameters based on the relevant OTUs (Schloss et al., 2009). Specifically, Chao1 and Shannon diversity indices were visualized applying OmicShare online tools (https://www.omicshare.com/tools), an online platform for data analysis. Rarefaction was analyzed using Mothur v1.43.0 and the curves were drawn applying the R vegan package (v2.5-6) (Schloss et al., 2009) Venn diagrams of the

SMCs were generated on Tutu Cloud website tool (http://www.cloudtutu.com/), a free online data calculation platform. Principal coordinate analysis (PCoA) was performed to determine community structure and *β*-diversityof RS microbes. Based on the Bray–Curtis distances calculated by estimating the number of OTUs, PCoA was performed using OmicShare tools (Gao *et al.*, 2019). Bar graphs of microbial community compositions at the phylum level based on their relative abundances (RAs) were generated using MS Excel 2016 (Microsoft Corp., Redmond, WA, USA). Heatmaps of SMCs at the genus level, and correlations between the SMC RAs and variables analyzed (plant growth, major bioactive components, and soil enzyme activities and physicochemical traits) were calculated and visualized applying OmicShare website tools (https://www.omicshare.com/tools). Co-occurrence networks of SMCs at the phylum level were visualized applying the Wekemo Bioincloud website tool (https://www.bioincloud.tech/task-meta), a free data analysis platform of the Wekemo Technology Co., Ltd., Shenzhen, Guangdong, China. The interrelationships among soil microbial characteristics (SMCs), soil properties, plant growth, and major bioactive components were analyzed using the Structural Equation Modeling (SEM) package in R environment (v4.5.1). The structural equation model was diagrammed using Microsoft PowerPoint 2021 (Microsoft Corp., Redmond, WA, USA).

In addition, the average values of plant growth parameters, artemisinin and total polyphenol contents, soil enzyme activities, and soil physicochemical properties at every growth stage of *A. annua* were calculated using MS Excel 2016 (Microsoft Corp., Redmond, WA, USA). Calculations were conducted using IBM Software SPSS Statistics v23.0 (IBM Corp., Armonk, NY, USA). Dissimilarities between mean parameters were analyzed by one-way analysis of variance (ANAOVA). A line graph of the analyzed parameters of *A. annua* was generated applying Microsoft Excel 2016 (Microsoft Corp., Redmond, WA, USA).

Results

Soil physicochemical traits and enzymatic activities at different growth stages of *A. annua*: Analysis of soil physicochemical properties revealed that soil OM, pH, AP, AN, and AK were decreased with the progression of *A. annua* growth. No significant dissimilarities were discovered in soil physicochemical traits between the two provenances (Figs. 1A–E). For instance, pH, OM, AN, AP, and AK of soils at the end of *A. annua* growth period (SP) obtained from GT were individually 12.77, 51.13, 31.57, 56.32, and 72.60 % lower than those at the initial stage (ST) of *A. annua* (Figs. 1A–E). Conversely, soil enzyme activities, including URA, PHA, and SUA were increased with the progression of *A. annua* growth stages, except for PHA during the SP stage, which was lower than that observed during the FBD stage. URA, PHA, and SUA in the soil of *A. annua* from provenance JC during the final growth stage were 3.36-, 2.33-, and 3.55-fold higher than those observed at the initial stage (Figs. 1F–H).

Soil URA was significantly negatively related to AN (regression equation was $y = -1.050x + 283.560$; *r*, -0.793; *n*, 27, *p*≤0.01). Soil PHA was significantly negatively correlated with AP (regression equation was $y = -0.0188x$

$+ 3.292$; *r*, -0.814, *n*, 27, *p*≤0.01). Soil SUA was significantly negatively related to OM ($y = -0.417x + 47.737$; *r*, -0.972, *n*, 27, *p*≤0.01).

Variations in plant growth parameters and contents of major bioactive components: Overall, the plant height, branch number, as well as artemisinin and total polyphenol contents were increased with the progression of *A. annua* growth (Fig. 2). No significant difference was observed in the four parameters during the SS stage. For *A. annua* obtained from provenance GT, the maximum plant height was 71.60 cm, number of branches was 28.04, and artemisinin and total polyphenol contents were individually 8.00 and 4.78 g kg^{-1}. For *A. annua* obtained from provenance JC, the maximum plant height was 93.56 cm, number of branches was 35.16, and artemisinin and total polyphenol contents were 3.45 g kg^{-1} and 4.75 g kg^{-1}, respectively. The number of branches in *A. annua* obtained from provenance GT during the FBD and SP stages were 25 and 28, respectively, which were 3 and 7, respectively, lower than those in *A. annua* obtained from provenance JC. However, the artemisinin content in *A. annua* obtained from provenance GT was 4.55 g kg^{-1} higher than that in *A. annua* obtained from provenance JC during the final stage (Figs. 2A–D).

Correlation analysis showed that *A. annua* growth, and artemisinin and total polyphenol contents were significantly negatively interplayed with soil physicochemical properties (pH, OM, AP, AN, and AK), but significantly positively correlated with soil enzyme activities (Table 1). For instance, significant negative linkages were observed between artemisinin content and soil pH (*r*, -0.85; *p*≤0.001), OM (*r*, -0.69; *p*≤0.001), AP (*r*, -0.83; *p*≤0.001), AN (*r*, -0.72; *p*≤0.001), AK (*r*, -0.70; *p*≤0.001), whereas significant positive relationships were discovered between artemisinin content and soil enzyme activities (URA *r*, 0.51, *p*≤0.01; PHA *r*, 0.72, *p*≤0.001; SUA *r*, 0.71, *p*≤0.001).

DNA sequences of soil microbial communities: A total of 2,846,389 valid reads and 168,017 OTUs were obtained for bacteria, and 3,634,155 valid reads and 16,101 OTUs for fungi (Table 2). Bacterial and fungal rarefaction curves of Shannon approached a saturation plateau (Figs. 3A & B), suggesting that the sequence data was reliable and represented most of the microbial species in the samples.

To estimate the commonality and particularity of SCMs, Venn diagrams were used to identify OTUs shared at different growth stages of *A. annua* obtained from two provenances. The numbers of OTUs shared by bacterial communities in soil samples obtained from provenances GT and JC were 4093 and 4238, respectively. The minimum numbers of unique OTUs were observed during the FBD stage (GT = 686 and JC = 696) of *A. annua* growth, while the maximum numbers of OTUs differed (Figs. 3C & D). The numbers of OTUs shared by fungal communities in soil samples obtained from provenances GT and JC were 288 and 285, respectively. The maximum numbers of unique OTUs were observed during the SP stage of *A. annua* growth (GT = 314 and JC = 332). However, the minimum numbers of OTUs differed, with 108 OTUs being observed at the SS stage for GT and 119 OTUs at the NF stage for JC (Figs. 3E & F). Generally, the total number of bacterial OTUs in the soil was decreased with the progression of *A. annua* growth. In contrast, the total fungal number of OTUs from the RS was increased with the growth progression of *A. annua* (Figs. 3C–F).
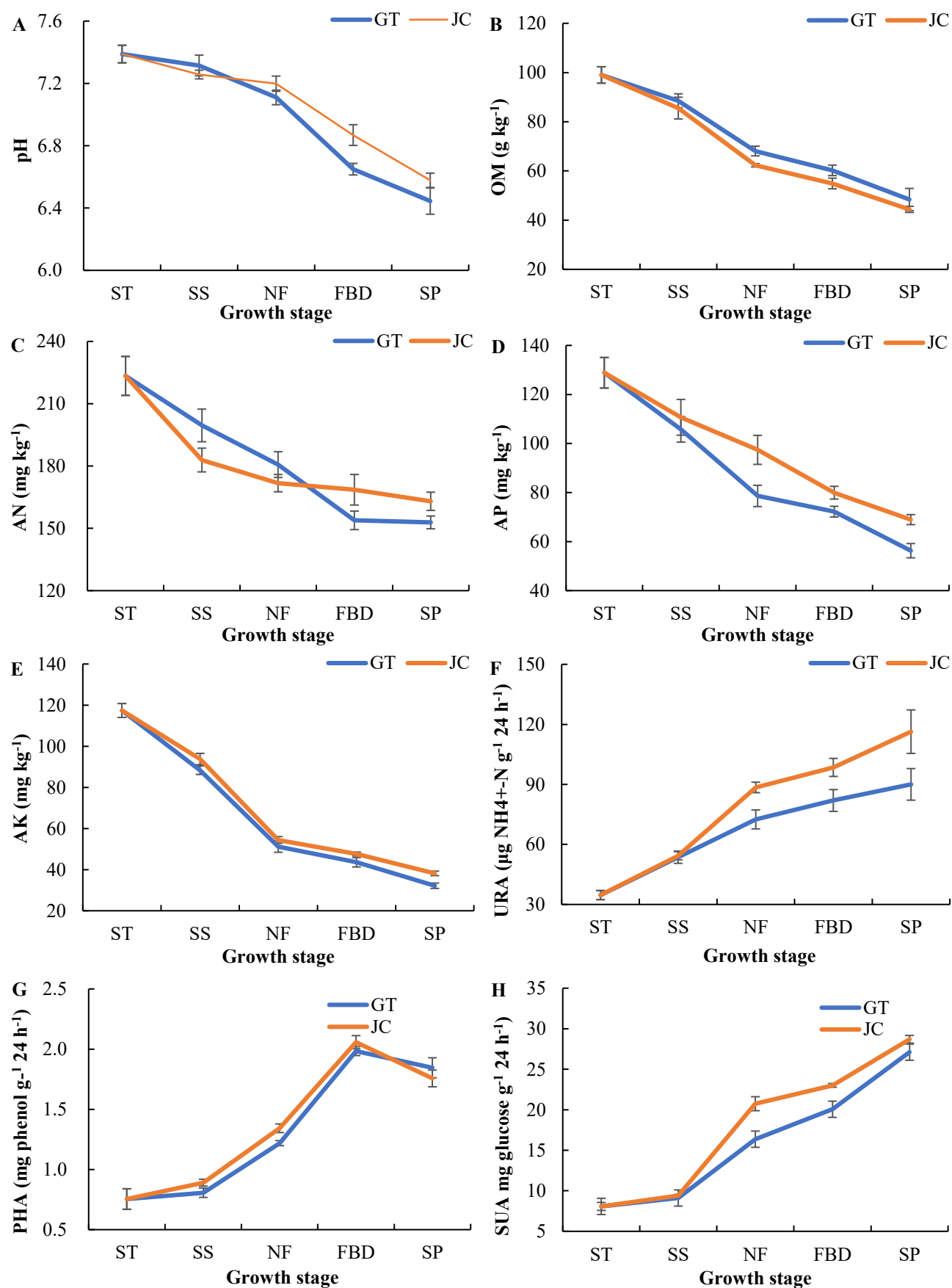
Fig. 1. Physicochemical traits and three enzymatic activities from potted soil at different growth stages of *A. annua* from two provenances (GT, Gaotun of Liping county; JC, Jiuchang of Guiyang City, Guizhou province, China) (x ± s, n = 3). A pH; B Organic matter (OM); C Available nitrogen (AN); D Available phosphorus (AP); E Available potassium (AK); F Urease activity (URA); G Phosphatase activity (PHA); H Sucrase activity (SUA). In periods of seed treatment (ST, sowing, control soil), seedling stage (SS, 15 days after the seedlings were transplanted to pots), nutritional flourish (NF), flower bud differentiation (FBD) and squaring period (SP) of *A. annua* plants, the samples were collected. The same as the following.
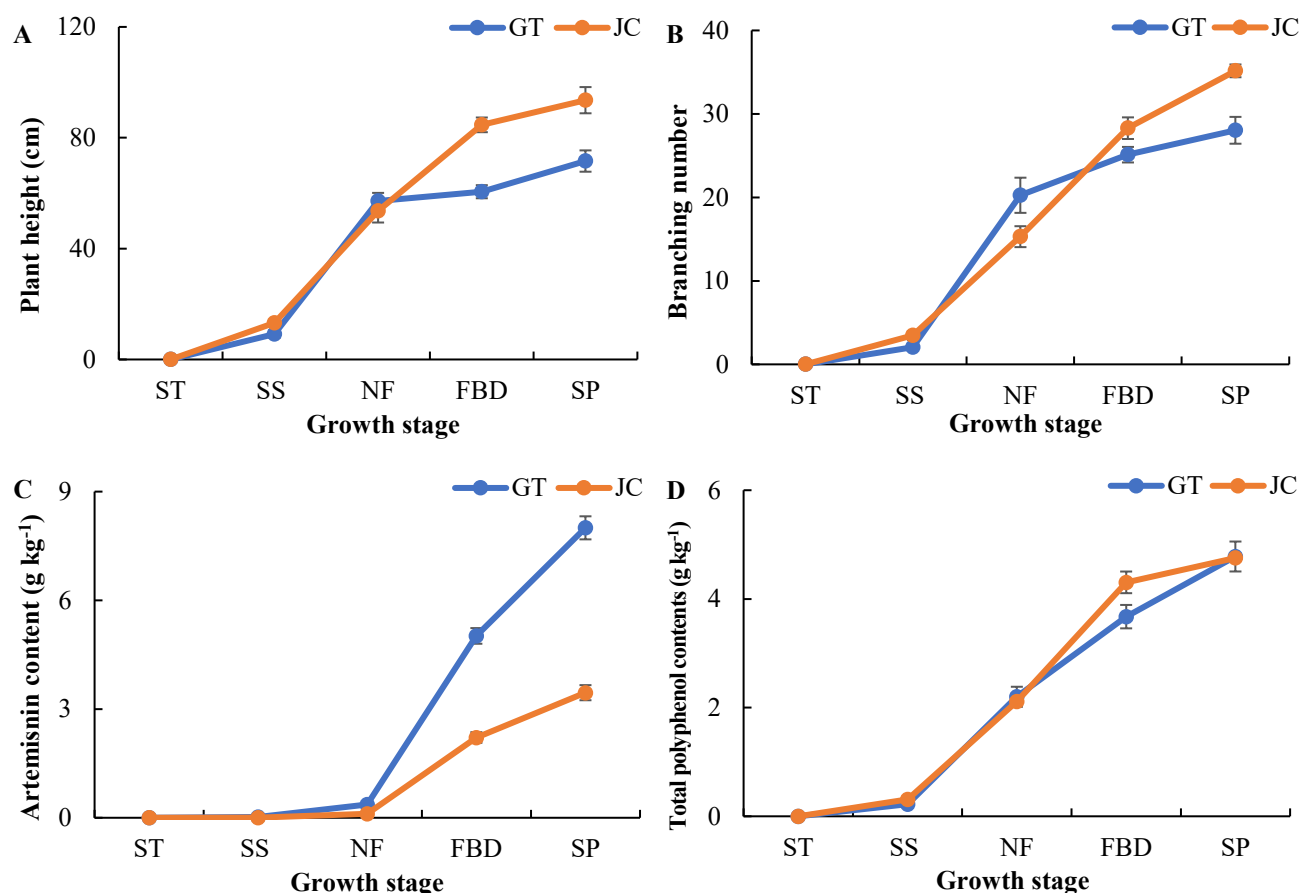
Fig. 2. Plant growth and the contents of artemisinin and total polyphenol in leaves during different growth periods of *A. annua*.

Soil microbial community structure and diversity: PCoA analysis results according to the Bray–Curtis coefficient revealed that the structure of the SMC varied in different stages of *A. annua* growth. According to PCoA1, the SMCs in the plant growth stages ST, SS, and NF were distinctly distinguished from FBD and SP, except for the Bray–Curtis coefficient of a NF-GT sample in the fungal community that was above zero, although PCoA2 did not reveal dissimilarities between soil bacterial and fungal communities at all growth stages of *A. annua* (Figs. 4A & B).

Analysis of OTUs revealed that the dominant bacterial phyla in the soil were Proteobacteria, Actinobacteria, Acidobacteria, Planctomycetes, Verrucomicrobia, Gemmatimonadetes, Bacteroidetes, Chloroflexi, Parcubacteria, and Armatimonadetes, which make up over 93% of the total relative abundance (RA) of bacteria at each growth stage (Fig. 4C). The RAs of Proteobacteria at *A. annua* NF stage were the highest (GT = 45.39% and JC = 48.43%), which were 13.69% (GT) and 16.73% (JC) higher than those at the ST stage, respectively. The top six phyla fungi were Ascomycota, Chytridiomycota, Mortierellomycota, Basidiomycota, Mucoromycota, and Glomeromycota comprising of more than 39.17% of the fungal total RA at each growth stage of *A. annua* (Fig. 4D). The RA of Ascomycota was the highest, and was higher at the FBD (GT = 74.28% and JC = 84.08%) and SP (GT = 71.21% and JC = 64.37%) stages than those at the ST (57.61%), SS (GT = 21.87% and JC = 46.03%), and NF (GT = 58.35% and JC = 49.53%) stages. The RA of bacterial Proteobacteria initially increased, and subsequently decreased, while RA of fungal Ascomycota

initially decreased and subsequently increased with the progression of *A. annua* growth.

The richness and *α*-diversity of bacteria and fungi in the RS of *A. annua* based on the number of OTUs are illustrated in Fig. 5. For provenance GT, Shannon and Chao1 indices for soil bacteria during the FDB and SP stages were considerably lower than those observed during the ST, SS, and NF stages (Figs. 5A & B). Shannon and Chao1 indices for soil fungi during the FDB and SP stages were considerably higher than those observed during the ST, SS, and NF stages (Figs. 5E & F). No significant dissimilarities were found in fungal and bacterial Shannon and Chao1 indices among ST, SS, and NF stages or between FBD and SP stages of GT provenance *A. annua* (Figs. 5A, B, E & F). For provenance JC, Shannon and Chao1 indices of soil bacteria generally decreased with the progression of *A. annua* growth stages, except for Chao1 at the SS stage (Figs. 5C & D). However, no significant differences were observed in Shannon indices of soil fungi at all growth stages. Chao1 index of soil fungi at the SP stage was significantly higher than those at the SS and NF stages, and its mean was the highest (Figs. 5G & H). Overall, soil bacterial diversity and richness decreased with the progression of *A. annua* growth, whereas fungal diversity and richness exhibited a contrasting trend.

Variations of soil microbial communities at different growth stages of *A. annua*: RAs above 0.1% of 33 bacteria and fungi communities at the genus level were individually analyzed and visualized based on OTUs using heatmaps, as presented in Fig. 6. The RAs of 9 bacterial genera during the ST stage of *A. annua* growth were greater than 1%, and the

RAs varied with the progression of *A. annua* growth and seed source (Fig. 6A). For instance, the RA of soil *Sphingomonas* from two provenances generally increased with the progression of *A. annua* growth stages, except its RA in SP stage was a little lower than FBD stage from JC. Seven bacterial genera *Streptomyces*, *Flavisolibacter*, *Altererythrobacter*, *Adhaeribacter*, *Nocardioides*, *Marmoricola*, and *Gemmatimonas* were similar with *Sphingomonas* in the RAs. On the contrary, the RA of *Pirellula* in soil from two provenances gradually decreased during the stages of *A. annua* growth, exception of r RA in NF stage from JC. A similar trend with *Pirellula* was observed for *Planctomyces*, *Opitutus*, *Chthoniobacter*, and RB41in the soil from GT. Additionally, the RAs of 20 genus bacteria varied at the different stages of *A. annua* growth.

In contrast to the ST stage, the RAs of some genus fungi during the FBD and SP stages increased considerably (Fig. 6B). The RAs of the genus fungi *Penicillium*, *Pestalotiopsis*, *Aspergillus*, *Talaromyces*, *Trichoderma*, *Cladosporium*, *Alternaria*, *Acrocalymma*, and *Gibberella* in soil at the FBD stage from provenance GT considerably higher than those observed at the ST stage, respectively. The RAs of the fungal genera *Acrocalymma*, *Metarhizium*, *Chaetomium*, *Plenodomus*, *Dactylonectria*, *Mycoleptodiscus*, *Edenia*, and *Myxosporea* at the SP stage from provenance GT were also differently fold higher than those observed at the ST stage. The RAs of the fungal genera *Cylindrocarpon*, *Metarhizium*, *Chaetomium*, *Plenodomus*, and *Dactylonectria* in soil at the FBD stage from provenance JC were varying-fold higher than those observed at the ST stage. The RAs of *Spizellomyces*, *Epicoccum*, *Ampelomyces*, *Bartalinia*, *Purpureocillium*, *Mycoleptodiscus*, and *Edenia* at the SP stage were also significantly higher than those at the ST stage. Overall, the heatmap results revealed that the RAs of bacteria and fungi communities varied at the different growth stages of *A. annua*.

Table 1. The Pearson correlations among plant growth, principally active components and soil properties, enzymatic activities (*n* = 27).

Parameters	pH	OM	AN	AP	AK	URA	PHA	SUA
Plant height	-0.74***	-0.86***	-0.73***	-0.72***	-0.82***	0.86***	0.83***	0.84***
Branching number	-0.92***	-0.94***	-0.84***	-0.89***	-0.92***	0.86***	0.91***	0.93***
Artemisinin	-0.85***	-0.69***	-0.72***	-0.83***	-0.70***	0.51**	0.72***	0.71***
Total polyphenol	-0.94***	-0.95***	-0.85***	-0.90***	-0.91***	0.86***	0.93***	0.95***

Note: *** Represent that the correlation between two parameters is highly significant at p≤0.001 level;
** Represent that the correlation significance is at *p*≤0.01 level

**Table 2. DNA sequence results of *A. annua* soil microbes.**

| Provenances	Sample names	Clean reads		OTUs	
		16S	ITS	16S	ITS
GT	ST-1	107766	156013	6439	458
	ST-2	101728	123621	6959	545
	ST-3	102523	146166	6617	419
	SS-1	97385	126322	6138	523
	SS-2	101223	129802	6712	598
	SS-3	108341	103720	6503	486
	NF-1	102454	132245	6340	579
	NF-2	95514	95203	6703	496
	NF-3	112031	121865	6715	574
	FBD-1	103326	151155	5572	740
	FBD-2	96266	164828	5271	745
	FBD-3	94379	148722	5536	695
	SP-1	112517	138341	6407	779
	SP-2	103846	150078	5401	736
	SP-3	101213	120193	5774	772
JC	SS-1	132217	120176	7496	535
	SS-2	115989	130940	7238	515
	SS-3	116186	113151	7279	545
	NF-1	111284	154160	6403	478
	NF-2	90430	121821	5775	544
	NF-3	109068	130604	6481	503
	FBD-1	104319	142933	5394	484
	FBD-2	100778	136575	6016	771
	FBD-3	94684	148424	5766	518
	SP-1	106258	154724	5457	687
	SP-2	112162	135081	5588	736
	SP-3	112502	137292	6037	640
Total		**2846389**	**3634155**	**168017**	**16101**
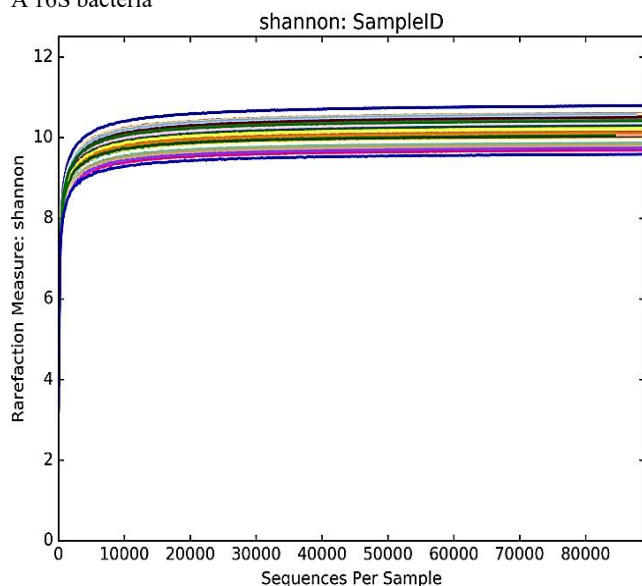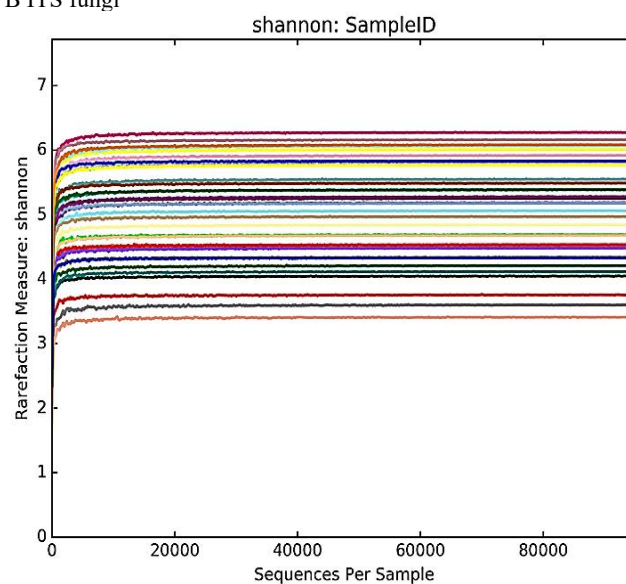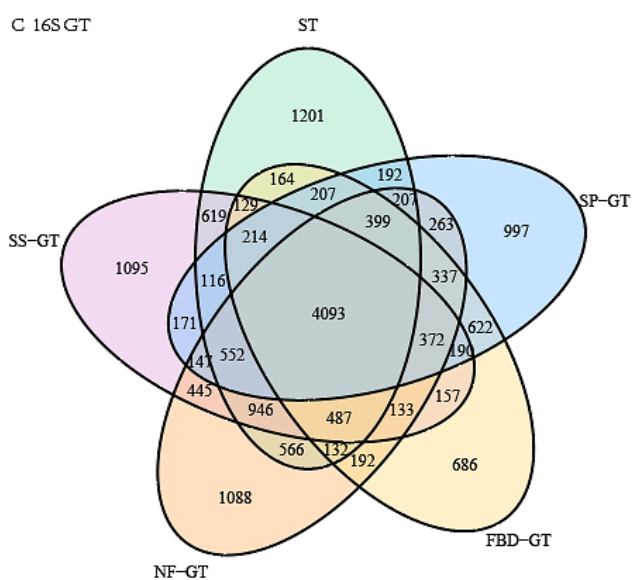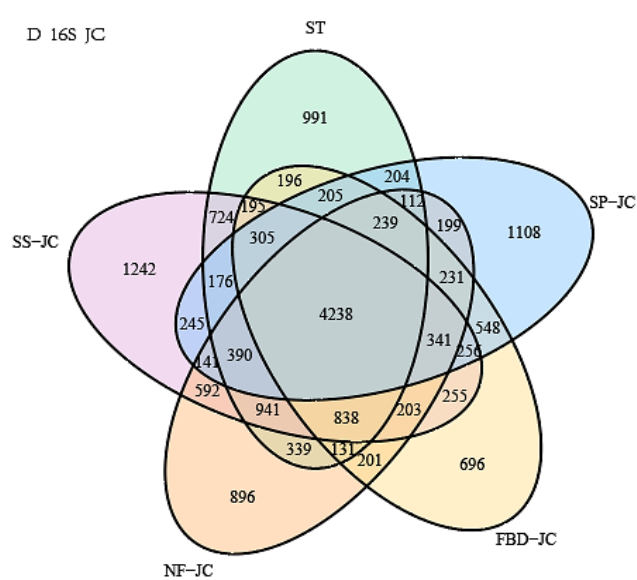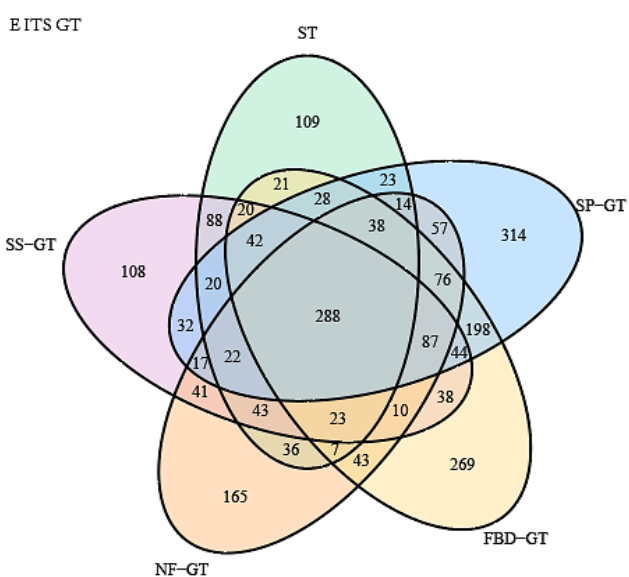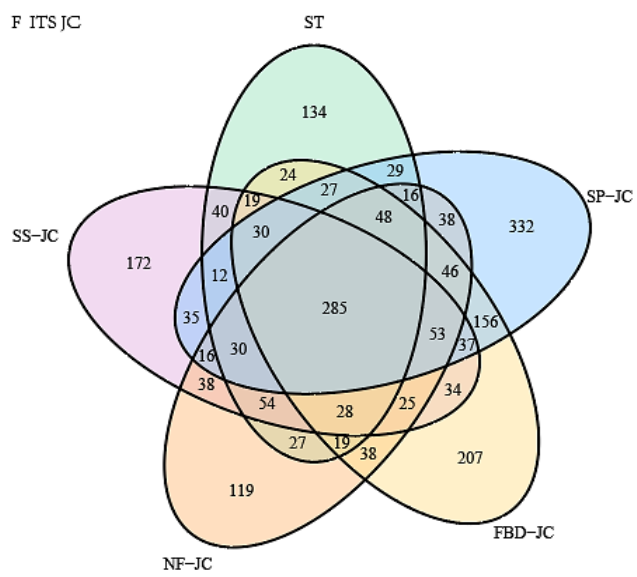
Fig. 3. Results of sequence from of all samples about bacterial and fungal OTUs of *A. annua* soil in different growth stage. A and B represent Shannon rarefaction curves of bacteria 16S and fungi ITS, respectively; C, D, E, F Venn diagram show the unique and shared soil bacterial and fungal OTUs of plants from GT, JC provenances, respectively.
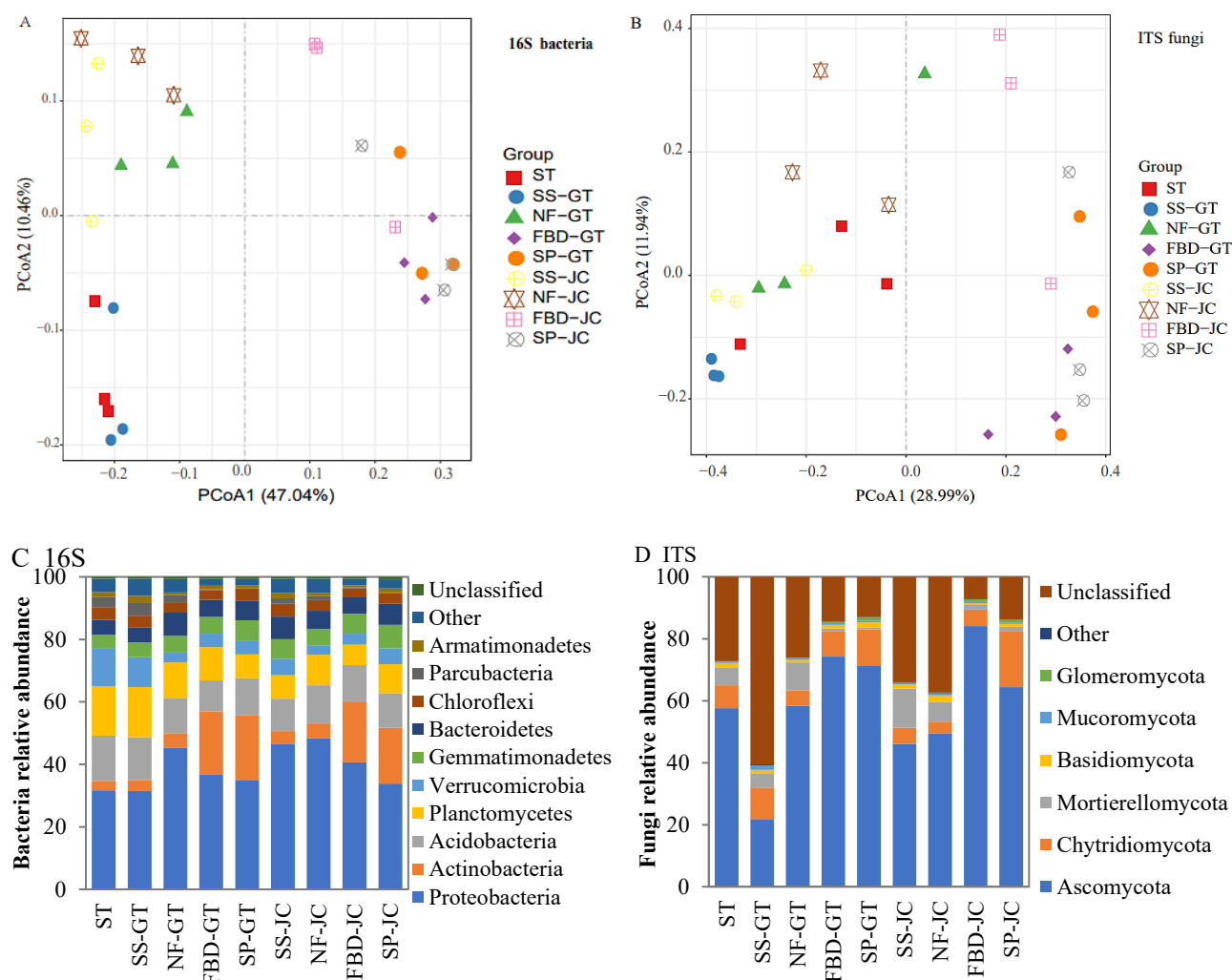
Fig. 4. Structure of soil bacteria and fungi communities in different growth stages of *A. annua*. A and B represent Principal coordinate analysis (PCOA) of soil bacteria and fungi OTUs, respectively; C and D represent the relative abundance of bacteria and fungi at Phylum level, respectively. Only proportion > 1% was exhibited in the figures.

Co-occurrence networks of SMCs at phylum level: Variations in SMC interactions in the RS of *A. annua* are presented (Fig. 7 & Fig. 8). Because no differences were observed in the microbial co-occurrence networks between provenances GT and JC soil across all the growth stages (Figs. 7A & B), the co-occurrence network data in every stage of *A. annua* growth were individually calculated using the RAs of soil bacterial and fungal communities from two provenances. The results revealed that variations in soil microbial co-occurrence networks at the different growth stages of *A. annua* were notable. Weaker microbial co-occurrence networks were observed during the SS, NF, FBD, and SP stages compared with ST stage (Figs. 8A–E). The maximum number of total network edges (172) and nodes (33 including 25 bacterial and 8 fungal nodes) were observed during the ST stage, followed by the SS (100 edges, 32 nodes including 24 bacterial and 8 fungal nodes) and FBD (65 edges, 31 nodes including 23 bacterial and 8 fungal nodes) stages. The minimum number of network nodes and edges were observed during the NF (31 edges and 25 nodes) and SP (30 edges and 29 nodes) stages. The average degree of the microbial networks showed the average node size, which indirectly represented the mean RA of all phylum SMCs when compared to the ST stage (10.42), where the average degrees observed at other growth stages

decreased to varying degrees (Fig. 8F). The minimum average degree of the microbial network was observed during the SP stage, which suggests that the average abundances of all phylum SMCs were decreased with the progression of *A. annua* growth. During the last SP stage, there was the highest positive correlation percentage (63.33%) and the lowest negative correlation rate (36.67%). While the correlation percentage in other growth stages were comparable, with nearly 54% positive correlation and 45 % negative correlation.

Correlations among SMCs and soil characteristics, plant growth, and major bioactive components: The analysis results of Pearson's correlation revealed that the RAs of 15 bacterial genera including *Streptomyces*, *Bryobacter*, *Sphingomonas*, *Nocardioides*, *Marmoricola*, *Iamia*, *Gemmatimonas*, *Flavisolibacter*, *Altererythrobacter*, Adhaeribacter, *Arenimonas*, *Gaiella*, *Caenimonas*, *Massilia*, and *Phenylobacterium* were significantly positively related to plant height, number of branches, total polyphenol and artemisinin contents, and soil enzyme activities (URA, SUA, and PHA) ($p<0.001$ or $p<0.01$ or $p<0.05$), except no significant correlation was observed between *Arenimonas* and soil SUA ($p\geq0.05$). However, their RAs were significantly negatively related to soil pH, AK, AP, AN, and

OM (*p*<0.001 or *p*<0.01 or *p*<0.05). The RAs of 11 bacterial genera *Planctomyces*, *Opitutus*, H16, SM1A02, *Hydrogenophaga*, *Pirellula*, *Devosia*, RB41, *Panacagrimonas*, *Herpetosiphon*, and *Nitrospira* were significantly negatively related to plant height, number of branches, total polyphenol and artemisinin contents, and soil enzyme activities (URA, SUA, and PHA) (*p*<0.001 or *p*<0.01 or *p*<0.05), except the correlation between H16 and plant height was not significant (*p*≥0.05). In contrast, the RAs of the 11 bacterial genera were significantly positively related to soil pH, AK, AP, AN, and OM (*p*<0.001 or *p*<0.01 or *p*<0.05), except the relationship between *Opitutus* and AP

was not significant. Furthermore, the RAs of Pir4_lineage, *Chtheoniobacter*, and *Lysobacter* were significantly correlated with certain parameters (*p*<0.05 or *p*<0.01 or *p*<0.001). For example, the relative abundance of Lysobacter was significantly negatively related to number of branches, total polyphenol and artemisinin contents, and SUA (*p*<0.001 or *p*<0.01 or *p*<0.05), but significantly positively related to soil pH, AK, AP, AN, and OM (*p*<0.001 or *p*<0.01 or *p*<0.05). The correlation results imply that most of the soil bacteria analyzed in this study had close relationships with soil traits, plant growth parameters, and major bioactive components of A. annua (Fig. 9A).
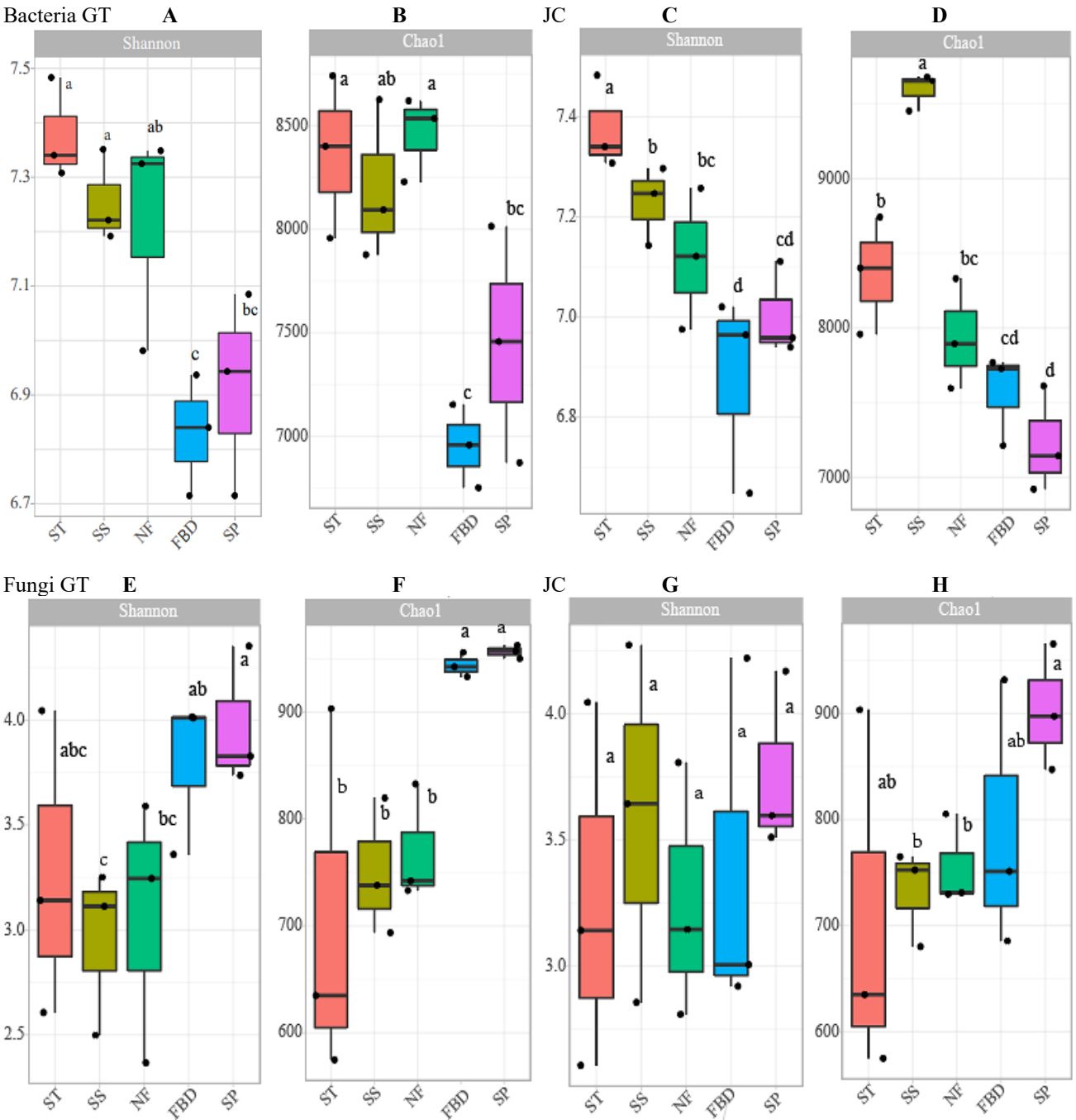
Fig. 5. α-diversity of soil bacteria and fungi communities in different growth stages of *A. annua*. A and B represent the bacteria Shannon and Chao1 from GT provenance soil, C and D represent Shannon and Chao1 of bacteria from JC provenance soil, respectively; similarly, E and F represent fungal Shannon and Chao1 indexes of GT, D and H represent fungal Shannon and Chao1 indexes in soil of JC, respectively. For all box plots, the central line represents the mean, different lowercase letters show significant difference (*p* ≤ 0.05) among growth stages based one-way ANOVA by Tukey's test.
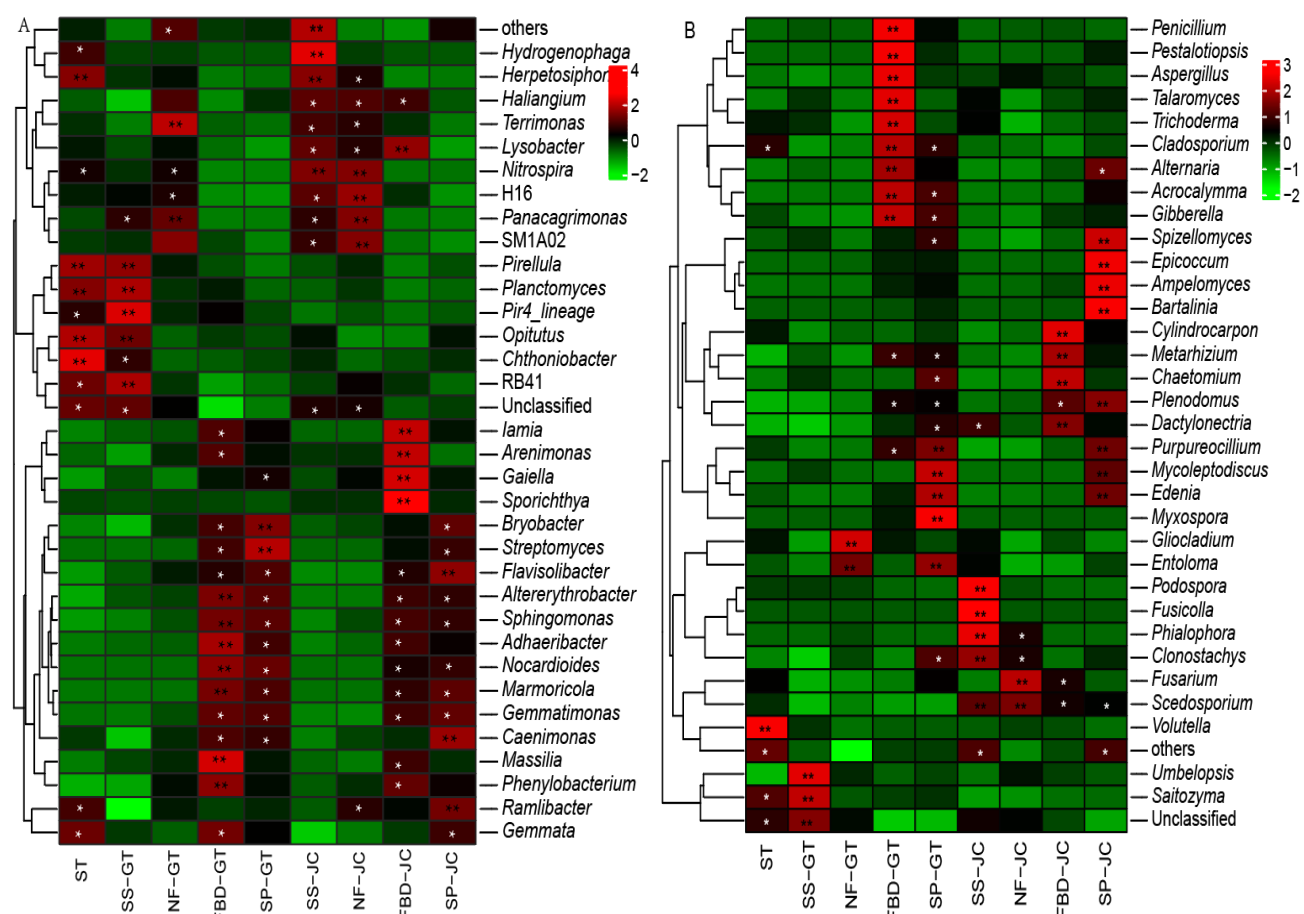
Fig. 6. Heatmap of bacterial and fungal communities at the genus level. A represents bacteria; B represents fungi. To read easy the heatmaps, bacteria and fungi genera in row were clustered according their relative abundance, respectively. ** present significant difference in the same row ($p \le 0.01$); * presents significant difference at 0.05 level in the same row ($p \le 0.05$).

Fig. 7. Networks of soil bacteria and fungi communities at phylum level two provenances of *A. annua*. Each node indicates one phylum, the node size indicates the degree. Bacterial nodes (blue circles), Fungal nodes (red circles). The edges are colored lines according to interaction types, positive correlations are showed with red lines, negative correlations are blue lines.

A ST   B SS   C NF

D FBD   E SP
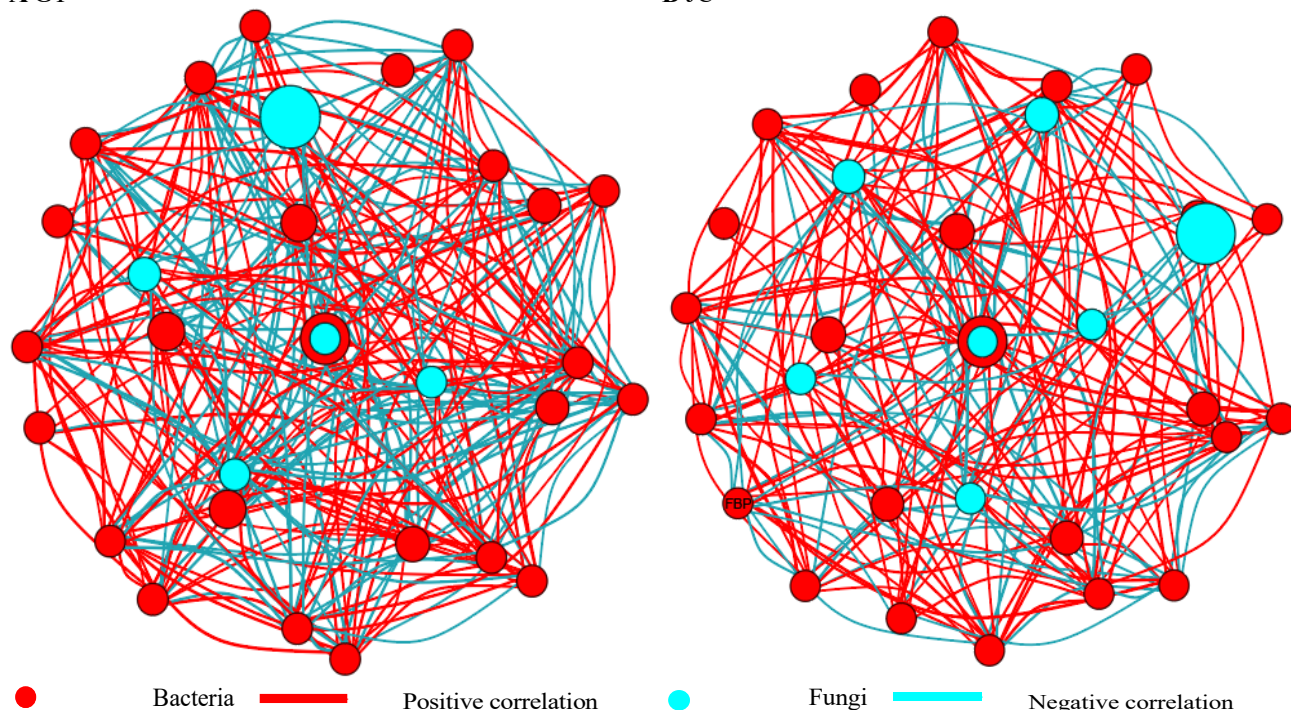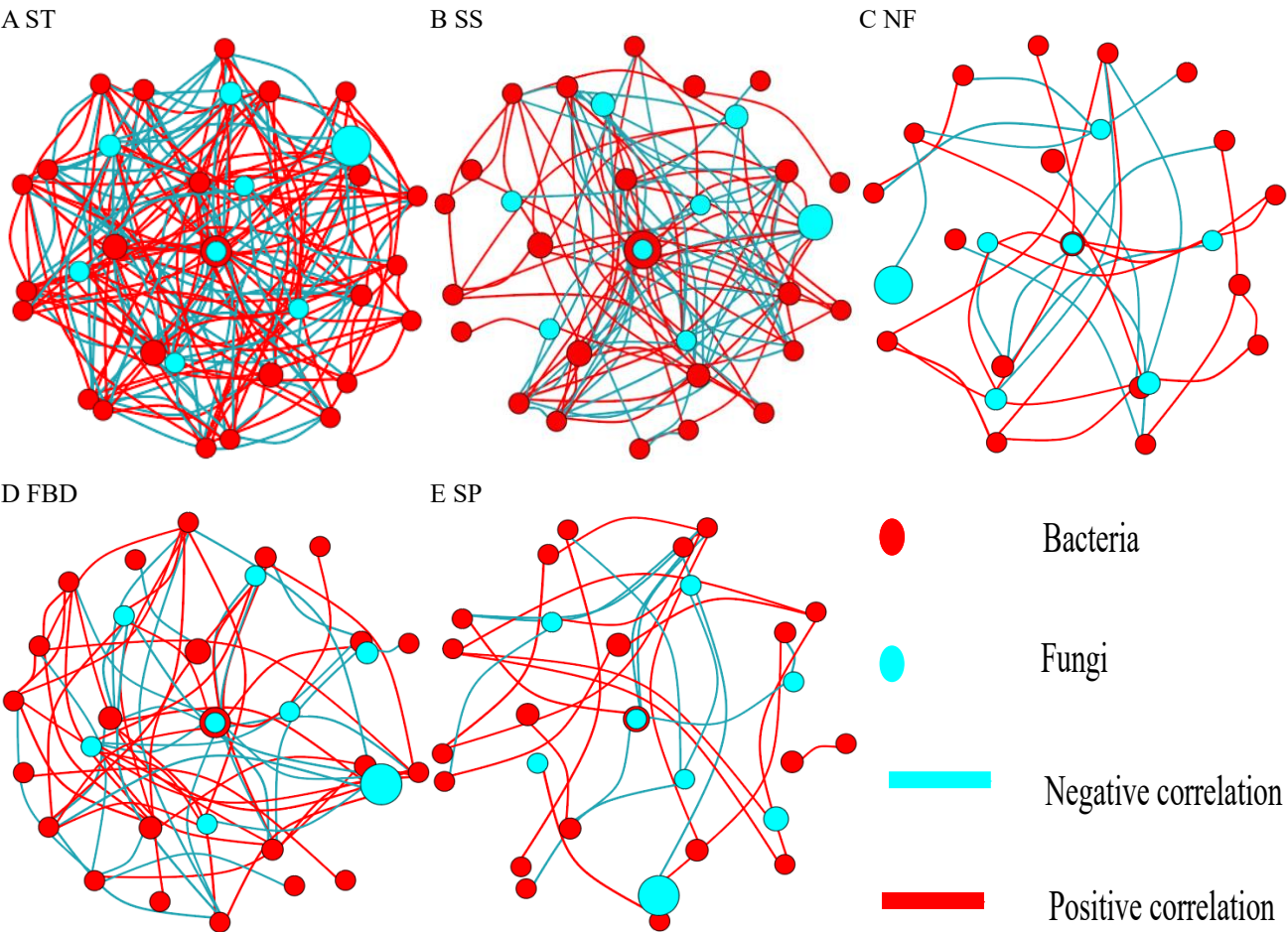

- Bacteria

- Fungi

- Negative correlation

- Positive correlation

F Parameters of networks

Plant growth stages	ST	SS	NF	FBD	SP
Average degree	10.42	6.25	2.48	4.19	2.06
Average closeness centrality	10.42	12.15	5.66	9.36	4.57
Average betweeness centrality	0	43.06	29.36	37.16	23.17
Bacteria nodes	25	24	18	23	21
Fungi nodes	8	8	7	8	8
Edges	172	100	31	65	30
Positive correlation percentage (%)	54.07	54.00	54.84	54.46	63.33
Negative correlation percentage (%)	45.93	46.00	45.16	46.54	36.67

Fig. 8. Networks of soil bacteria and fungi communities at phylum level in different growth stages of *A. annua*. Each node indicates one phylum, the node size indicates the degree. Bacterial nodes (red circles), Fungal nodes (blue circles). The edges are colored lines according to interaction types, positive correlations are showed with red lines, negative correlations are blue lines.

Although most of the RAs of 33 fungi at the genus level in this study were not correlated with RS physicochemical traits, soil enzymatic activities, parameters of plant growth, and contents of these major bioactive components, some strong correlations were observed. The RA of *Plenodomus* had significant positive relationships with plant height, number of branches, total polyphenol and artemisinin contents, and soil enzyme activities (URA, SUA, and PHA) ($p<0.001$), but significantly negatively correlated with soil pH, AK, AP, AN, and OM ($p<0.001$ or $p<0.01$). The RA of *Metarhizium* was significantly positively correlated with plant height, number of branches, total polyphenol and artemisinin contents, and two soil enzyme activities (URA and PHA) ($p<0.01$ or $p<0.05$), but significantly negatively correlated with soil pH, AK, AP, AN, and OM ($p<0.05$). The RAs of *Purpureocillium*, *Edenia*, *Alternaria*, and *Acrocalymma* had significant positive correlations with the number of branches, total polyphenol and artemisinin

contents, and two soil enzyme activities (SUA and PHA) ($p<0.01$ or $p<0.05$), but significant negative relationships with soil pH, AK, AP, AN, and OM ($p<0.01$ or $p<0.05$). The RAs of fungi *Spizellomyces*, *Epicoccum*, and *Ampelomyces* were significantly positively related to plant height, number of branches, total polyphenol and artemisinin contents, and soil SUA ($p<0.01$ or $p<0.05$), but significantly negatively related to soil pH, AP, and OM ($p<0.01$ or $p<0.05$). However, no significant relationship was found between artemisinin content and the RA of *Epicoccum*. In addition, the RAs of fungal *Gibberella*, *Mycoleptodiscus*, *Myxosporea*, *Penicillium*, and *Cladosporium* were significantly positively correlated with artemisinin content ($p<0.01$ or $p<0.05$), and those of *Dactylonectria*, *Cylindrocarpon*, and *Gibberella* were significantly positively related to PHA. Significant negative relationships ($p<0.05$) were uncovered between soil pH and the RAs of *Gibberella* and *Myxosporea*, and between AP and *Gibberella* (Fig. 9B).
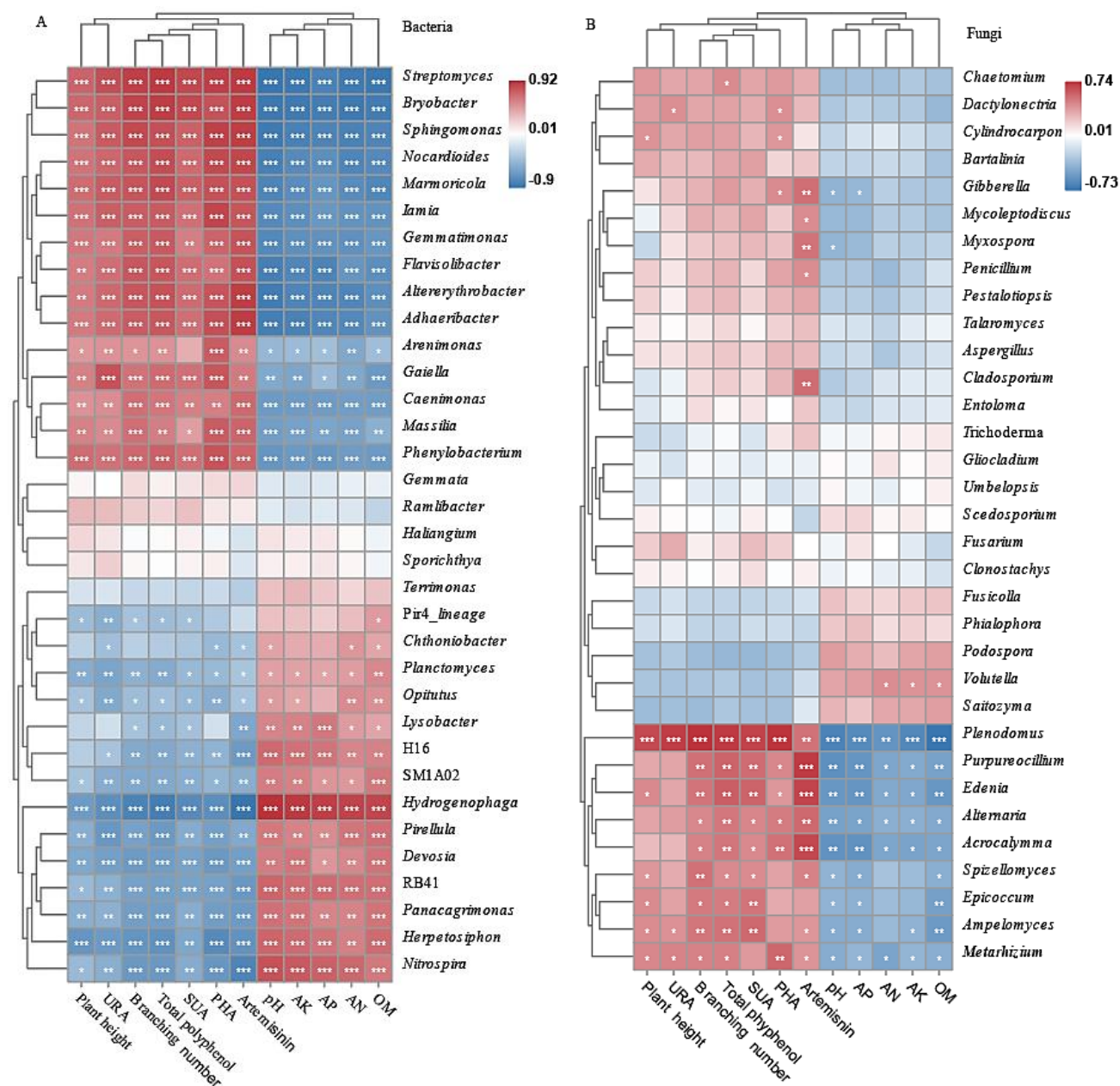
Fig. 9. Correlation among relative abundance of microbe communities and indexes. A represents relationships of soil bacteria and every index; B represents relationships of soil fungi and every index. The bacteria and fungi with any repetition over 0.1% are shown in the Fig. 8A and B. 27 repetitions were used to calculate the relationship coefficients (Pearson). No significance $p \geq 0.05$ was not labeled with *; significance $p < 0.001$ was labeled with***, $p < 0.01$ **, $p < 0.05$ *.

The structural equation model (SEM) constructed to evaluate the interrelationships among microbial abundance, soil properties, plant growth, and major bioactive components showed a good fit with the observed data (Fisher's C = 3.14, P = 0.208, df = 2), indicating that the proposed conceptual framework is consistent with the empirical data (Fig. 10). Path analysis revealed that soil enzyme activities, while most strongly negatively influenced by soil chemical properties (standardized total coefficient = –0.803, $p < 0.001$), exerted the strongest positive effect on plant growth (standardized total coefficient = 0.595, $p < 0.05$). Although soil enzyme activities did not show statistically significant effects on microbial abundance or major active components, however, a slight positive tendency was observed. In contrast, soil

chemical properties had a significant negative direct effect on major bioactive components (standardized total coefficient = –0.547, $p < 0.05$). While their direct effects on microbial abundance and plant growth were not statistically significant, soil chemical properties still exhibited weak negative relationships with both. Similarly, the total microbial abundance (including both bacteria and fungi) showed modest negative associations with plant growth and the synthesis of major active components, although these pathways were also not significant (Fig. 10). Additionally, Chao 1 and Shannon indexes of rhizosphere bacteria were significantly correlated with the growth, the contents of total polyphenol and artemisinin, while Chao 1 index was significantly related to the growth and the active components of *A. annuna* (Table 3).

Fisher's C = 3.14, *P* = 0.208 , df = 2 , * *P* < 0.05, ** *P* < 0.01, *** *P* < 0.001

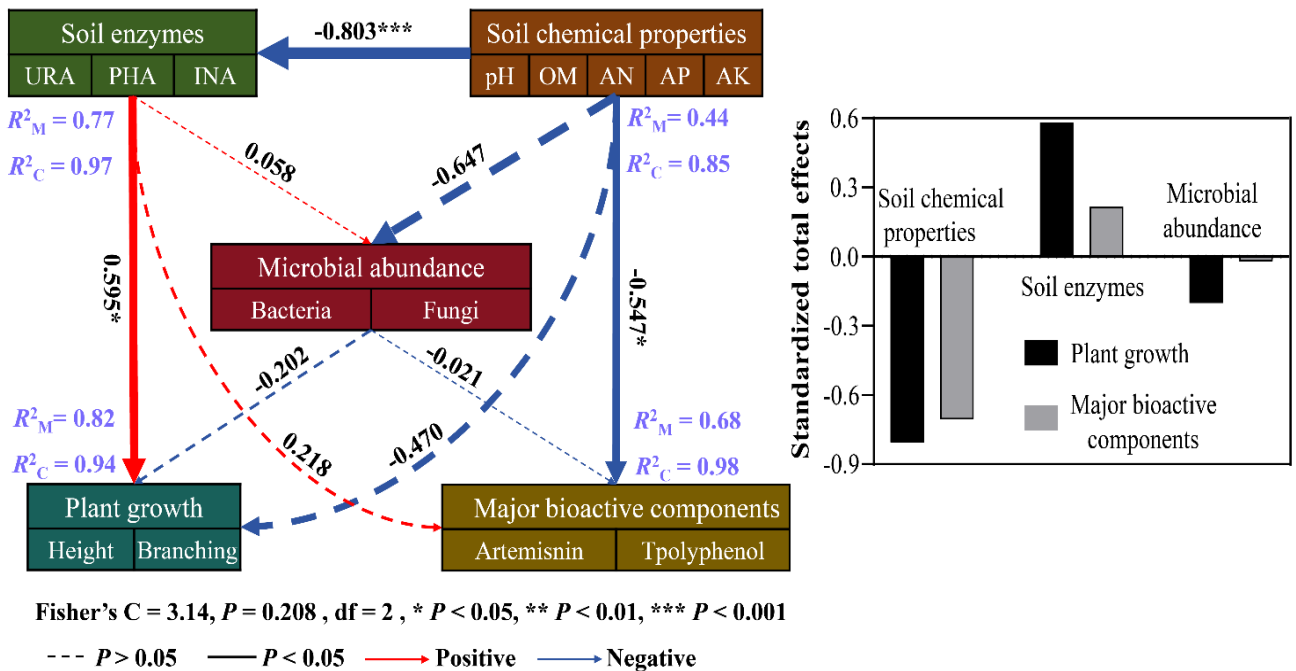- - - *P* > 0.05   ——— *P* < 0.05   ——→ Positive   ——→ Negative

Fig. 10. The structural equation model (SEM) illustrates the relationships among microbial abundance, soil chemical properties, soil enzyme activities, plant growth, and major bioactive components. The conditional (C) and marginal (M) R^2 represent the proportion of variance explained by all factors. Solid arrows indicate significant paths ($p<0.05$), while dashed arrows indicate non-significant paths ($p>0.05$). The numbers adjacent to the lines are the standardized path coefficients, indicating the degree of standard deviation change in dependent variables when each independent variable changes by one standard deviation. The color of the arrows denotes the nature of the relationship: red for positive and blue for negative. The arrow width is proportional to the strength of the relationship. Significance levels: non-significance ($p>0.05$) is not labeled with *; significance $p<0.001$ is labeled with ***, $p<0.01$ with **, and $p<0.05$ with *. Standardized total effects of key factors on plant growth and major bioactive components from the SEM analysis.

Table 3. The Correlation of plant growth, main active components and soil microbial alpha diversity of *A. annua* ($n = 27$).

Diversity indices	Bacteria		Fungi	
	Chao1	**Shannon**	**Chao1**	**Shannon**
Plant height	-0.54**	-0.52**	0.43*	0.17
Branching number	-0.69***	-0.68***	0.60***	0.35
Total polyphenol	-0.72***	-0.72***	0.66***	0.36
Artemisinin	-0.65***	-0.66***	0.76***	0.50*

Notes: *** represent that the correlation between two parameters is highly significant at $p\leq0.001$ level; ** represent the correlation significance is at $p\leq0.01$ level; * represents the correlation significance is at $p\leq0.05$ level
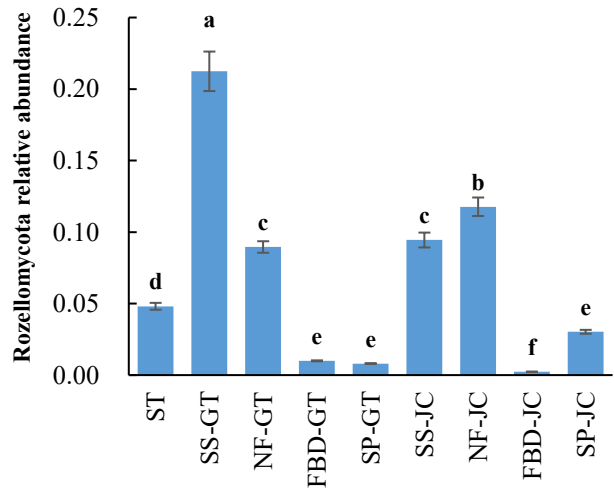
Fig. 11. The relative abundance of fungal Phylum Rozellomycota in different growth stages of *A. annua* from two provenances (x ± s, *n* = 3).

Discussion

Variations in soil microbial diversity at different stages of *A. annua* growth: The diversity of SMCs at different stages of *A. annua* growth varied correspondingly. Variations in bacterial *α*-diversity in the RS of growing plants have been reported in numerous plants, including sorghum (*Sorghum bicolor* L. Moench), sunflower (*Helianthus annuus* L.), wheat (*Triticum aestivum* L.) and rice (*Oryza sativa* L.) (Panico *et al*., 2020; Wang *et al*., 2018a). However, in our experience, soil bacterial *α*-diversity, which was based on Shannon and Chao1 indices, decreased during the last two growth stages (FBD and SP stages) of *A. annua* when compared to the first three stages (ST, SS, and NF), and soil microbial diversity patterns between the two provenances were similar (Figs. 5A–D). Conversely, soil fungal diversity was increased during the FBD and SP stages (except for the Shannon diversity during SS stage for provenance JC) (Figs.5E–H). This could be due to the increased active components secreted by *A. annua*,

thereby suppressing the growth of some bacteria (Liu *et al.*, 2018). For example, Artemisinin and polyphenol contents in the *A. annua* plant were negatively related to the bacterial genera such as *Hydrogenophage*, *Pirellua*, and *Devosia* so on (Fig. 9A), these active components may be secreted into the soil by *A. annua* root and inhibit the bacterial growth. The opposite is true for some fungi, such as *Edenia, Altemaria, and Acrocalymma* so on (Fig. 9B), which further affected the diversity and richness.

Fluctuations in soil microbial communities at different growth stages of *A. annua*: The composition of SMCs fluctuated with the *A. annua* growth progression. The RAs of the phylum bacteria Proteobacteria and Acidobacteria have been shown to increase in soil planted with *A. annua* when compared to unplanted soil (Shi *et al.*, 2021). In our experiment, RA of the bacterial phylum, Proteobacteria, which accounted for 31.45–48.43% of the bacteria, initially increased and then decreased from the ST to SP stages. The maximum RA was observed at the NF stage in both provenances (Fig. 4C). Proteobacteria are associated with carbohydrate metabolism and carbon assimilation, which enhance plant growth (Trivedi *et al.*, 2013; Philippot *et al.*, 2013; Liao, 2009). The Acidobacteria RA (2.99–20.83%) generally increased with the progression of *A. annua* growth. Acidobacteria is involved in sulfur (S) metabolism, polysaccharide hydrolysis, and hydrogen oxidation (Hausmann *et al.*, 2018), which promote the C and S cycling, in turn, enhancing plant growth. The Verrucomicrobia RA is generally reduced with the progression of *A. annua* growth (Fig. 4C) in spite of its polysaccharide metabolism ability (Sichert *et al.*, 2020). Similarly, the RAs of 10 bacterial genera (including *Bryobacter*, *Streptomyces*, *Flavisolibacter*, *Altererythrobacter*, *Sphingomonas*, *Adhaeribacter*, *Nocardioides*, *Marmoricola*, *Gemmatimonas*, and *Caenimonas*) raised during the FBD and SP stages (Fig. 6A). For example, *Sphingomonas* consists of bacterial species that protect plants against attack by pathogenic fungus and promote plant growth (Wang *et al.*, 2023; Luo *et al.*, 2019c), in this study, the RA of this bacterial genus in FBD and SP stages were considerably higher than the former three growth stages of *A. annua*.

A previous report uncovered that the abundance of the fungus, Rozellomycota phylum in the RS under a 7-year plantation of *A. annua* in Guangxi province of China was increased, but the abundance of Ascomycota was decreased (Shi *et al.*, 2021). In our study, although the RA of Rozellomycota (Fig. 11) was considerably lower than that of Shi's report, the abundance of this phylum and other certain fungal communities fluctuated. Additionally, the RA of the fungus, Ascomycota phylum (21.9–84.1%,) was initially decreased considerably from the ST to SS stages, subsequently increased sharply from the SS to FBD stages, and finally decreased from the FBD to SP stages. A parallel trend was found for Chytridiomycota; however, the Mortierellomycota RA exhibited a contrasting trend (Fig. 4D). The fluctuations in the RAs could be associated with multiple factors, including soil traits, nutrients, climatic conditions, planting time and others, which lead to variation in microbial species recruitment (Petipas *et al.*,

2021; Oldroyd & Leyser, 2020; Panico *et al.*, 2020). At the genus level, the RAs of the fungal genera varied with the growth stages of *A. annua* and provenance, which is inconsistent with the report of Shi *et al.*, (2021). Our results suggest that *A. annua* has adaptation to a wide range of conditions and can recruit different microbial species from the surrounding soil.

Variations in microbial co-occurrence networks at different stages of *A. annua* growth: According to the analysis results of microbial co-occurrence network, simpler soil bacterial and fungal interplay networks were observed at the phylum level during the SS, NF, FBD, and SP stages than those during the ST (CK) stage of *A. annua* growth (Fig. 8). The finding is consistent with the observation made by Shi *et al.*, (2021) that fungal and bacterial networks in the RS of *A. annua* were simpler than those in unplanted RS. Similar results have been found in other plants, for example, the wheat RS has less complex microbial networks than bulk soil (Fan *et al.*, 2018). Multiple factors could have contributed to the less complex microbial networks. In the pot experiments, the plant root system occupied a considerable proportion of the soil with growing plants, the soil was nutrient-rich with readily available resources, such as enzymes secreted by soil microbes (Staudinger *et al.*, 2021; Huang *et al.*, 2022) and plants, and photosynthates exuded by the root system (Mencuccini & Hölttä, 2009). Soil enzymes facilitate the transformation of organic matter into inorganic substances, which enhances the absorption of nutrients for plant. The extra nutrients reduce dependency and competition for resources among soil microbes, which supports more free-living microbial communities with simpler networks in the rhizosphere soil (Hubbell, 2005).

Correlations among SMCs, soil properties, and plant parameters: Soil microbes are closely associated with soil properties, and they influence nutrient cycling and organic matter transformation through multiple biophysical and biochemical mechanisms, in turn, altering soil properties and microbiome assembly (Philippot *et al.*, 2023). In our work, the RAs of 11 RS bacterial communities were significantly positively related to soil pH, AK, AP, AN, and OM, whereas those of 15 soil bacterial communities had significant negative relationship with soil pH, AK, AP, AN, and OM (Fig. 9A). However, significant negative correlations were observed between the RAs of 11 soil fungi and soil pH, between the RAs of 10 soil fungi and AP, between the RAs of 6 soil fungi and AN, between the RAs of seven soil fungi and AK, between the RAs of 9 soil fungi and OM, as well as significant positive correlations were found between the RAs of the soil fungal genus, *Volutella* and AN, AK, and OM (Fig. 9B). The correlation analysis revealed that soil bacteria had more positive correlations than soil fungi, in spite of some negative relationships that were found between SMCs and soil traits. Significant positive correlations were observed between the RAs of 15 soil bacterial communities and soil enzyme activities (URA, SUA, and PHA) (Fig. 9A), between the relative abundances of 4 soil fungi and URA, between the relative abundances of 8 soil fungi and SUA, and between the

relative abundances of 9 soil fungi and PHA (Fig. 9B). These results suggested that these soil microbes secreted extracellular enzymes or promoted soil enzyme activities. Significant negative correlations were found between the relative abundances of 13 soil bacteria and URA and SUA, as well as between the RAs of 12 soil bacteria and PHA (Fig. 9A). The correlation analysis suggested that not all SMCs contributed to the enhancement of soil enzyme activity.

Plants absorb nutrients from the soil during their growth to ensure healthy growth and development (Oldroyd & Leyser, 2020). In our study, pot experiments with water management and no fertilization treatments were performed, and soil nutrients were not supplemented during the experimental period. According to the results, soil OM, AN, AP, and AK decreased with the progression of *A. annua* growth (Figs. 1B–E), which could be because plant growth leads to the absorption of soil nutrients. Soil pH decreased with the progression of *A. annua* growth (Figs. 1A). Organic acids secreted from growing plant roots increase soil acidity (Yang *et al.*, 2020). The release of CO_2 and hydrogen protons by plant roots through root and soil respiration also decreases soil pH (Xie *et al.*, 2022). Soil enzyme activities (URA, PHA, and SUA) were increased with the progression of *A. annua* growth, which could be conductive to the augment of enzymes secreted from the growing plant roots (Wang *et al.*, 2018a). Accumulation of extracellular enzymes secreted by soil microorganisms (Schimel & Schaeffer, 2012), in addition to increased soil temperatures could enhance the soil enzymatic activities (Regan *et al.*, 2014). Nevertheless, soil URA, SUA, and PHA were significantly negatively correlated with AN, OM, and AP contents, respectively, it is inconsistent with the results of earlier researches (Nwe *et al.*, 2023; Wang *et al.*, 2018b). We speculate that the quantities of AN, OM, and AP absorbed by *A. annua* exceeded those produced through enzymatic hydrolysis, but the real mechanism need to be further studied.

The interactions between RS and plant roots form specific soil environments around plant roots, and affect the composition of SMCs (Koorem *et al.*, 2020; Smith *et al.*, 2018), with certain soil microbes having close associations with plants (Xiao *et al.*, 2017). Previous researchers have studied the interactions between soil properties and microbes (Pii *et al.*, 2015; Edwards *et al.*, 2015; Peiffer *et al.*, 2013; Lundberg *et al.*, 2012). Xiao *et al.*, (2017) investigated the relationship between plant biomass and soil microbiome. The results of the present study showed that the relative abundances of 15 soil bacteria were significantly positively correlated with plant height and number of branches (Fig. 9A). Bacterial genera, including *Streptomyces*, *Sphingomonas*, *Nocardioides*, and *Flavisolibacter*, are related to the promotion of plant growth (Meena *et al.*, 2023; Omar *et al.*, 2022; Asaf *et al.*, 2020). The bacterial genus *Iamia* is associated with smut resistance in sugarcane (*Saccharum officinarum* L.) (Duan *et al.*, 2023). *Gemmatimonas* is associated with nitrous oxide reduction (Park *et al.*, 2017). Significant positive correlations were uncovered between the RAs of seven soil fungal genera and plant height, and between the RAs of nine soil fungal genera and the branches number. A previous study reported that treatment of soil with 10 and

20 mg kg^{-1} of artemisinin substantially decreased soil microbial biomass, species richness (Chao1 and ACE), and Shannon diversity indexes (Liu *et al.*, 2018). In this work, significant negative correlations were observed between the RAs of 13 soil bacterial genera and artemisinin and total polyphenol contents (Fig 9A), which could be attributed to the inhibition of bacterial growth and development by artemisinin and polyphenols secreted by *A. annua* roots (Fig. 9A). A previous study showed that 20 and 40 mg L^{-1} of artemisinin inhibited the growth of inorganic phosphate-solubilizing bacteria and P solubility in the soil (Luo *et al.*, 2013), in addition to inhibiting the growth and N-fixing capacity of *Rhizobium* associated with *Vigna* species (Li *et al.*, 2011). Certainly, some soil microbial communities were not sensitive to the bioactive components of *A. annua* possibly, it might be because the contents were not high enough to inhibit soil microbial growth. In our experiment, the RAs of 15 soil bacterial genera had significant positive linkages with artemisinin and total polyphenol contents in *A. annua* leaves (Fig. 9A). It was also possible that these bacteria were able to antagonize other microorganisms, thereby inhibiting the growth of certain bacteria (e.g. the previous 13 bacteria) making them as dominant communities.

Plant height and branch number of *A. annua* were increased with the progression of plant growth, and the parameters were significantly negatively correlated with soil physicochemical properties (pH, OM, AN, AK, and AP). This could be due to the absorption of available nutrients in the soil by the growing plants, which in turn, led to a decrease in available nutrients in the soil. In contrast, plant height and number of *A. annua* branches were significantly positively correlated with soil URA, SUA, and PHA, implying that the amount of soil enzymes secreted by plant roots increased as the plants continued to grow. Similarly, the contents of major bioactive components increased with the progression of *A. annua* growth, with the maximum artemisinin and total polyphenol contents being observed during the SP stage (Figs. 2C & D), which is in accordance with previous researches (Zhu *et al.*, 2010; Gu *et al.*, 2008; Li *et al.*, 2007). So, we hypothesized that the rate of photosynthesis was increased with the progression of *A. annua* growth, leading to the accumulation of organic compounds and increased synthesis of artemisinin and polyphenols. Furthermore, artemisinin content of *A. annua* from provenance GT (8.00 g kg^{-1}) was substantially higher than that of *A. annua* from provenance JC (3.45 g kg^{-1}) during the SP stage. Artemisinin content of *A. annua* from provenance GT exceeded the minimum requirements for industrial extraction (5 g kg^{-1}, Wei *et al.*, 2008), thereby meeting the standard value for industrial utilization.

Conclusion

According to this study, fluctuations in microbial communities in the soil of *A. annua* were not affected by seed provenances, although they were correlated with plant growth and development. Co-occurrence networks of SMCs with the progression of *A. annua* growth stages became less complex. The structure of microbial community observed in the later development stages (FBD

and SP) differed from the initial development stages (SS, NF, and FBD). Moreover, the diversity and richness of the fungal community boosted with the progression of *A. annua* growth, whereas the diversity and richness of the bacterial community were reverse. The artemisinin content of *A. annua* from provenance GT was higher than that of *A. annua* from provenance JC and exceeded the recommended industrial extraction standards. The RAs of certain bacteria and fungi were significantly positively related to the growth and the artemisinin content. Nevertheless, the present study is not without its limitations. Firstly, the dynamics of the soil bacterial and fungal communities were the sole focus of the study. Secondly, the anti-malaria artemisinin content was determined in the main active ingredients only. Further studies should extend the mechanism exploration of interaction between microbial functional genes and other active ingredients. Even with these limitations, our findings provide insights into the relationships among plant agronomic traits, bioactive components, and soil microbial communities, and provide a theoretical foundation for further exploration of plant-associated microorganisms and sustainable cultivation of medicinal plants.

Abbreviations and shorthand notations: OM, Organic matter; pH, power of hydrogen; AN, available nitrogen; AP, available phosphorus; AK, available potassium; URA, urease activity; PHA, phosphatase activity; SUA, sucrase activity; ST, seed treatment period (sowing, CK); SS, seedling stage (15 days after the seedlings were transplanted to pots); NF, nutritional flourish, FBD, flower bud differentiation period; SP, squaring (bud emergence) period. GT, Gaotun of Liping county, Guizhou province, China; JC, Jiuchang of Guiyang City, Guizhou province, China. GC-MS, gas chromatograph-mass spectrometer; AGE, agarose gel electrophoresis; RS, Rhizosphere soil; RA, relative abundance; SMC, soil microbial community.

Statements & Declarations

Authors Contribution: Chu Yang: Performing the pot experiment, Validation, Data Visualization and curation, Outline. Hong-hao Huo: Performing the pot experiment, Validation. Shi-qiong Luo: Writing - original manuscript, Resources, Funding acquisition, Validation, Writing - review and editing; Zhan-nan Yang: Methodology, Validation, Writing - review and editing.

Competing Interests: The authors declare that they have no known competing financial interests or personal relationships that could have appeared to influence the work reported in this paper.

Acknowledgments

References

Abarenkov, K., R.H. Nilsson, K.H. Larsson, I.J. Alexander, U. Eberhardt, S. Erland, K. Høiland, R. Kjøller, E. Larsson, T. Pennanen, R. Sen, A.F. Taylor, L. Tedersoo, B.M. Ursing, T. Vralstad, K. Liimatainen, U. Peintner and U. Kõljalg. 2010. The UNITE database for molecular identification of fungi-recent updates and future perspectives. *New Phytol.*, 186(2): 281-285.

Anonymous. 2018. *World malaria report.* World Health Organization, Geneva.

Anonymous. 2020. Committee of Chinese Pharmacopoeia. *Chinese pharmacopoeia.* Vol: China Medical Science and Technology Press, Beijing.

Asaf, S., M. Numan, A.L. Khan and A. Al-Harrasi. 2020. Sphingomonas: from diversity and genomics to functional role in environmental remediation and plant growth. *Crit. Rev. Biotechnol.*, 40(2): 138-152.

Bao, S. 2000. *Soil agrochemical analysis.* Vol: China Agriculture Pree, Beijing.

Bardgett, R.D. and W.H. Van Der Putten. 2014. Belowground biodiversity and ecosystem functioning. *Nature*, 515: 505-511.

Bergmann, J., E. Verbruggen, J. Heinze, D. Xiang, B. Chen, J. Joshi and M.C. Rillig. 2016. The interplay between soil structure, roots, and microbiota as a determinant of plant-soil feedback. *Ecol. Evol.*, 6(21): 7633-7644.

Bjørnlund, L., M. Liu, R. Rønn, S. Christensen and F. Ekelund. 2012. Nematodes and protozoa affect plants differently, depending on soil nutrient status. *Eur. J. Soil Biol.*, 50: 28-31.

Clarholm, M., U. Skyllberg and A. Rosling. 2015. Organic acid induced release of nutrients from metal-stabilized soil organic matter–The unbutton model. *Soil Biol. Biochem.*, 84: 168-176.

Coskun, D., D.T. Britto, W. Shi and H.J. Kronzucker. 2017. How plant root exudates shape the nitrogen cycle. *Trends Plant Sci.*, 22(8): 661-673.

Duan, M., L. Wang, X. Song, X. Zhang, Z. Wang, J. Lei and M. Yan. 2023. Assessment of the rhizosphere fungi and bacteria recruited by sugarcane during smut invasion. *Braz. J. Microbiol.*, 54(1): 385-395.

Edgar, R.C. 2013. UPARSE: highly accurate OTU sequences from microbial amplicon reads. *Nat. Methods*, 10: 996-998.

Edgar, R.C. 2016. SINTAX: a simple non-Bayesian taxonomy classifier for 16S and ITS sequences. *bioRxiv.*

Edwards, J., C. Johnson, C. Santos-Medellín, E. Lurie, N.K. Podishetty, S. Bhatnagar, J.A. Eisen and V. Sundaresan. 2015. Structure, variation, and assembly of the root-associated microbiomes of rice. *PNAS*, 112(8): E911-E920.

Fan, K., P. Weisenhorn, J.A. Gilbert and H. Chu. 2018. Wheat rhizosphere harbors a less complex and more stable microbial co-occurrence pattern than bulk soil. *Soil Biol. Biochem.*, 125: 251-260.

Gao, F., Y.W. Lv, J. Long, J.M. Chen, J.M. He, X.Z. Ruan and H.B. Zhu. 2019. Butyrate Improves the metabolic disorder and gut microbiome dysbiosis in mice induced by a high-fat diet. *Front. Pharmacol.*, 10: 1040.

Goldsmith, C., H.D. Alexander, J.J. Granger and C.M. Siegert. 2023. Invasive *Microstegium vimineum* (Japanese stiltgrass) hinders growth and biomass of hardwood seedlings regardless of light and moisture regime. *Forest Ecol. Manag.*, 539: 120984.

Gu, A.Y., S.P. Li, L.Y. Yang, X. Wang, L. Li, B. Yang and S.W. Yan. 2008. Study on the optimal harvest time and drying methods of *Artemisia annua* L. in Yunnan province. *Southwest China J. Agric. Sci.*, 21(6): 1682-1684.

Guan, S.Y. 1986. *Soil Enzyme and Its Research Methods.* Vol: China Agriculture Pree, Beijing.

Guo, L., M. Ya, Y.S. Guo, W.L. Xu, C.D. Li, J.P. Sun, J.J. Zhu and J.P. Qian. 2019. Study of bacterial and fungal community structures in traditional koumiss from Inner Mongolia. *J. Dairy Sci.*, 102(3): 1972-1984.

Hausmann, B., C. Pelikan, C.W. Herbold, S. Köstlbacher, M. Albertsen, S.A. Eichorst, T. Glavina Del Rio, M. Huemer, P.H. Nielsen, T. Rattei, U. Stingl, S.G. Tringe, D. Trojan, C. Wentrup, D. Woebken, M. Pester and A. Loy. 2018. Peatland *Acidobacteria* with a dissimilatory sulfur metabolism. *ISME J.*, 12(7): 1729-1742.

Huang, Q., H. Liu, J. Zhang, S. Wang, F. Liu, C. Li and G. Wang. 2022. Production of extracellular amylase contributes to the colonization of *Bacillus cereus* 0–9 in wheat roots. *BMC Microbiol.*, 22(1): 205.

Hubbell, S.P. 2005. Neutral theory in community ecology and the hypothesis of functional equivalence. *Funct. Ecol.*, 19(1): 166-172.

Koorem, K., B.L. Snoek, J. Bloem, S. Geisen, O. Kostenko, M. Manrubia, K.S. Ramirez, C. Weser, R.A. Wilschut and W.H. Van Der Putten. 2020. Community-level interactions between plants and soil biota during range expansion. *J. Ecol.*, 108(5): 1860-1873.

Kourtev, P.S., J.G. Ehrenfeld and M. Häggblom. 2003. Experimental analysis of the effect of exotic and native plant species on the structure and function of soil microbial communities. *Soil Biol. Biochem.*, 35(7): 895-905.

Lau, J.A. and J.T. Lennon. 2012. Rapid responses of soil microorganisms improve plant fitness in novel environments. *PNAS*, 109(35): 14058-14062.

Li, C.H., L. Wang, B. He, W. Feng, J. Tian and H. Ai. 2007. Artemisinin content measuration of different growth and harvest period. *Lishizhen Med. Mater. Med. Res.*, 18(4): 888-889.

Li, Q., Y. Wu and J. Huang. 2011. Studies on allelopathic effect of artemisinin on rhizobium. *China J. Chin. Mate. Med.*, 36(24): 3428-3433.

Liao, F. 2009. Discovery of Artemisinin (Qinghaosu). *Molecules*, 14(12): 5362-5366.

Likhanov, A., M. Oliinyk, N. Pashkevych, A. Churilov and M. Kozyr. 2021. The role of flavonoids in invasion strategy of *Solidago canadensis* L. *Plants*, 10(8): 1748.

Liu, H., J. Huang and L. Yuan. 2018. *In vitro* effect of artemisinin on microbial biomasses, enzyme activities and composition of bacterial community. *Appl. Environ. Microbl.*, 124: 1-6.

Lundberg, D.S., S.L. Lebeis, S.H. Paredes, S. Yourstone, J. Gehring, S. Malfatti, J. Tremblay, A. Engelbrektson, V. Kunin, T.G.D. Rio, R.C. Edgar, T. Eickhorst, R.E. Ley, P. Hugenholtz, S.G. Tringe and J.L. Dangl. 2012. Defining the core *Arabidopsis thaliana* root microbiome. *Nature*, 488(7409): 86-90.

Luo, S.Q., C. Zhao, Z.N. Yang, J. Hu and S.J. Di. 2019b. Soil microbes and medical metabolites of *Artemisia annua* L. along altitudinal gradient in Guizhou Karst terrains of China. *J. Plant Interact.*, 14: 167-176.

Luo, S.Q., C. Zhao, Z.N. Yang, S.J. Di, Z. Zheng and J. Hu. 2019a. Correlation analysis of nutrients, enzymes, and microbial biomass in soils with phenolics of *Artemisia annua* L. *Pak. J. Agric. Sci.*, 56(1): 171-178.

Luo, S.Q., J. Huang and L. Yuan. 2014. Nutrients and microorganisms in soils with wild *Artemisia annua* L. *Acta Pedol. Sin.*, 51(4): 868-879.

Luo, S.Q., Y.Y. Ling and J. Huang. 2013. *In vitro* effects of artemisinin on inorganic phosphate- solubilizing bacteria. *Afr. J Microbiol. Res.*, 7(6): 525-532.

Luo, Y., F. Wang, Y. Huang, M. Zhou, J. Gao, T. Yan, H. Sheng and L. An. 2019c. *Sphingomonas* sp. Cra20 increases plant growth rate and alters rhizosphere microbial community structure of *Arabidopsis thaliana* under drought stress. *Front. Microbiol.*, 10: 1221.

Martin, M. 2011. Cutadapt removes adapter sequences from high-throughput sequencing reads. *EMBnet J.*, 17(1): 10-12.

Meena, K.K., A.M. Sorty, U. Bitla, A.L. Shinde, S. Kumar, G.C. Wakchaure, S. Kumar, M. Kanwat and D.P. Singh. 2023. Stress-responsive gene regulation conferring salinity tolerance in wheat inoculated with ACC deaminase producing facultative methylotrophic actinobacterium. *Front. Plant Sci.*, 14: 1249600.

Mencuccini, M. and T. Hölttä. 2009. The significance of phloem transport for the speed with which canopy photosynthesis and belowground respiration are linked. *New Phytol.*, 185(1): 189-203.

Nguyen, C. 2003. Rhizodeposition of organic C by plants: mechanisms and controls. *Agronomie*, 23(5-6): 375-396.

Nwe, T.Z., N.I. Maaroufi, E. Allan, S. Soliveres and A. Kempel. 2023. Plant attributes interact with fungal pathogens and nitrogen addition to drive soil enzymatic activities and their temporal variation. *Funct. Ecol.*, 37(3): 564-575.

Oldroyd, G.E.D. and O. Leyser. 2020. A plant's diet, surviving in a variable nutrient environment. *Science*, 368(6484): eaba0196.

Omar, A.F., A.H.A. Abdelmageed, A. Al-Turki, N.M. Abdelhameid, R.Z. Sayyed and M. Rehan. 2022. Exploring the plant growth-promotion of four *Streptomyces* strains from rhizosphere soil to enhance cucumber growth and yield. *Plants*, 11(23): 3316.

Ordoñez, J.C., P.M. Van Bodegom, J.P.M. Witte, R.P. Bartholomeus, H.F. Van Dobben and R. Aerts. 2010. Leaf habit and woodiness regulate different leaf economy traits at a given nutrient supply. *Ecology*, 91(11): 3218-3228.

Panico, S.C., F. Esposito, V. Memoli, L. Vitale, F. Polimeno, V. Magliulo, G. Maisto and A. De Marco. 2020. Variations of agricultural soil quality during the growth stages of sorghum and sunflower. *Appl. Soil Ecol.*, 152: 103569.

Park, D., H. Kim and S. Yoon. 2017. Nitrous oxide reduction by an obligate aerobic bacterium, *Gemmatimonas aurantiaca* strain T-27. *Appl. Environ. Microbl.*, 83(12): e00502-e00517.

Peiffer, J.A., A. Spor, O. Koren, Z. Jin, S.G. Tringe, J.L. Dangl, E.S. Buckler and R.E. Ley. 2013. Diversity and heritability of the maize rhizosphere microbiome under field conditions. *PNAS*, 110(6): 6548-6553.

Petipas, R.H., M.A. Geber and J.A. Lau. 2021. Microbe-mediated adaptation in plants. *Ecol. Lett.*, 24(7): 1302-1317.

Philippot, L., C. Chenu, A. Kappler, M.C. Rillig and N. Fierer. 2023. The interplay between microbial communities and soil properties. *Nat. Rev. Microbiol.*, 22(4): 226-239.

Philippot, L., J.M. Raaijmakers, P. Lemanceau and W.H. Van Der Putten. 2013. Going back to the roots: The microbial ecology of the rhizosphere. *Nat. Rev. Microbiol.*, 11(11): 789-799.

Pii, Y., L. Borruso, L. Brusetti, C. Crecchio, S. Cesco and T. Mimmo. 2015. The interaction between iron nutrition, plant species and soil type shapes the rhizosphere microbiome. *Plant Physiol. Bioch.*, 99: 39-48.

Poudel, A.S., P.K. Jha, B.B. Shrestha and R. Muniappan. 2019. Biology and management of the invasive weed *Ageratina adenophora* (Asteraceae): current state of knowledge and future research needs. *Weed Res.*, 59: 79-92.

Pytlarz, E. and D. Gala-Czekaj. 2022. Possibilities of using seed meals in control of herbicide-susceptible and -resistant biotypes of rye brome (*Bromus secalinus* L.) in Winter Wheat. *Plants*, 11(3): 331.

Regan, K.M., N. Nunan, R.S. Boeddinghaus, V. Baumgartner, D. Berner, S. Boch, Y. Oelmann, J. Overmann, D. Prati, M. Schloter, B. Schmitt, E. Sorkau, M. Steffens, E. Kandeler and S. Marhan. 2014. Seasonal controls on grassland microbial biogeography: Are they governed by plants, abiotic properties or both? *Soil Biol. Biochem.*, 71: 21-30.

Roscher, C., J. Schumacher, A. Lipowsky, M. Gubsch, A. Weigelt, S. Pompe, O. Kolle, N. Buchmann, B. Schmid and E.D. Schulze. 2013. A functional trait-based approach to understand community assembly and diversity–productivity relationships over 7 years in experimental grasslands. *Perspect. Plant Ecol.*, 15(3): 139-149.

Schimel, J.P. and S.M. Schaeffer. 2012. Microbial control over carbon cycling in soil. *Front. Microbiol.*, 3: 348.

Schloss, P.D., S.L. Westcott, T. Ryabin, J.R. Hall, M. Hartmann, E.B. Hollister, R.A. Lesniewski, B.B. Oakley, D.H. Parks, C.J. Robinson, J.W. Sahl, B. Stres, G.G. Thallinger, D.J. Van Horn and C.F. Weber. 2009. Introducing mothur: open-source, platform-independent, community-supported software for describing and comparing microbial communities. *Appl. Environ. Microbiol.*, 75(23): 7537-7541.

Schmieder, R. and R. Edwards. 2011. Quality control and preprocessing of metagenomic datasets. *Bioinformatics*, 27(6): 863-864.

Shi, Y., Y. Pan, L. Xiang, Z. Zhu, W. Fu, G. Hao, Z. Geng, S. Chen, Y. Li and D. Han. 2021. Assembly of rhizosphere microbial communities in *Artemisia annua*: recruitment of plant growth-promoting microorganisms and inter-kingdom interactions between bacteria and fungi. *Plant Soil*, 470: 127-139.

Sichert, A., C.H. Corzett, M.S. Schechter, F. Unfried, S. Markert, D. Becher, A. Fernandez-Guerra, M. Liebeke, T. Schweder, M.F. Polz and J.H. Hehemann. 2020. *Verrucomicrobia* use hundreds of enzymes to digest the algal polysaccharide fucoidan. *Nat. Microbiol.*, 5(8): 1026-1039.

Smith, M.E., J.M. Facelli and T.R. Cavagnaro. 2018. Interactions between soil properties, soil microbes and plants in remnant-grassland and old-field areas: a reciprocal transplant approach. *Plant Soil*, 433: 127-145.

Staudinger, C., B.M. Dissanayake, O. Duncan and A.H. Millar. 2021. The wheat secreted root proteome: Implications for phosphorus mobilisation and biotic interactions. *J. Proteomics*, 252: 104450.

Trivedi, P., I.C. Anderson and B.K. Singh. 2013. Microbial modulators of soil carbon storage: integrating genomic and metabolic knowledge for global prediction. *Trends Microbiol.*, 21(12): 641-651.

Van Der Heijden, M.G., R.D. Bardgett and N.M. Van Straalen. 2008. The unseen majority: Soil microbes as drivers of plant diversity and productivity in terrestrial ecosystems. *Ecol. Lett.*, 11(3): 296-310.

Wang, J., G. Rhodes, Q. Huang and Q. Shen. 2018a. Plant growth stages and fertilization regimes drive soil fungal community compositions in a wheat-rice rotation system. *Biol. Fertil. Soils*, 54: 731-742.

Wang, L., B. Otgonsuren, W. Duan and D. Godbold. 2018b. Comparison of root surface enzyme activity of ericaceous plants and *Picea abies* growing at the tree line in the Austrian Alps. *Forests*, 9(9): 575.

Wang, Y., Z.N. Yang and S.Q. Luo. 2023. An assembled bacterial community associated with *Artemisia annua* L. causes plant protection against a pathogenic fungus. *Front. Microbiol.*, 14.

Wei, S.G., X.J. Ma, S.X. Feng, R.S. Huang, Q.S. Dong, Z.G. Yan and Q.Y. Huang. 2008. Evaluation on germplasm resources of main production area of *Artemisia annua* in China. *China J. Chin. Mate. Med.*, 33(3): 241-244.

Xiao, X., M. Fan, E. Wang, W. Chen and G. Wei. 2017. Interactions of plant growth-promoting rhizobacteria and soil factors in two leguminous plants. *Appl.Microbiol. and Biotechnol.*, 101(23-24): 8485-8497.

Xie, Y., Y. Ouyang, S. Han, J. Se, S. Tang, Y. Yang, Q. Ma and L. Wu. 2022. Crop rotation stage has a greater effect than fertilisation on soil microbiome assembly and enzymatic stoichiometry. *Sci. Total Environ.*, 815: 152956.

Xu, D., E. Xiao, P. Xu, L. Lin, Q. Zhou, D. Xu and Z. Wu. 2017. Bacterial community and nitrate removal by simultaneous heterotrophic and autotrophic denitrification in a bioelectrochemically-assisted constructed wetland. *Bioresour. Technol.*, 245(Pt A): 993-999.

Yang, T.Y., Y.P. Qi, H.Y. Huang, F.L. Wu, W.T. Huang, C.L. Deng, L.T. Yang and L.S. Chen. 2020. Interactive effects of pH and aluminum on the secretion of organic acid anions by roots and related metabolic factors in *Citrus sinensis* roots and leaves. *Environ. Pollut.*, 262: 114303.

Yuan, Y., W. Zhao, J. Xiao, Z. Zhang, M. Qiao, Q. Liu and H. Yin. 2017. Exudate components exert different influences on microbially mediated C losses in simulated rhizosphere soils of a spruce plantation. *Plant Soil*, 419: 127-140.

Zhang, J., K. Kobert, T. Flouri and A. Stamatakis. 2013. PEAR: a fast and accurate Illumina Paired-End reAd mergeR. *Bioinformatics*, 30(5): 614-620.

Zhu, W., Z. Liu and X. Sheng. 2010. Dynamic changes on artemisinin contents and yields of *Artemisia annua* in different developmental stages and different level branches. Chinese J. *Chin. J. Mod. Appl. Pharm.*, 27(9): 805-808.